Subjects and Methods

Study Population

Between April 2005 and May 2006, 830 women underwent general health screening (Ningen Dock) including carotid ultrasonography as a part of the health screening course, and were enrolled in the present study. The study was approved by The Ethical Committee of Mitsui Memorial Hospital and University of Tokyo, Faculty of Medicine.

Laboratory Analysis

Blood samples were taken from the subjects after an overnight fast. Serum levels of total cholesterol, HDL-cholesterol, and triglycerides were determined enzymatically. Serum uric acid was measured by the uricase-peroxidase method, hemoglobin A_{1C} was determined using the latex agglutination immunoassay, and creatinine was determined by the enzymatic method. Plasma glucose was measured by the hexokinase method and serum insulin was measured by enzyme immunoassay. Homeostasis model assessment insulin resistance (HOMA-IR) was calculated in these individuals according to the following formula: HOMA-IR = [fasting immunoreactive insulin (μU/ml) × fasting plasma glucose (FPG; mg/dl)]/405.

Creatinine and urine albumin were measured by TBA-200FR (Toshiba Medical Systems, Tochigi, Japan) and by Accute (Toshiba Medical Systems), respectively, using commercially available kits, Accuras Auto CRE (Shino-test, Tokyo, Japan) and IATRO U-ALB (TIA) (Mitsubishi Kagaku Iatron, Tokyo, Japan), respectively. Serum creatinine was calibrated using the following formula: serum creatinine (Jaffe method) = 0.2 + serum creatinine (enzyme method). GFR was estimated by equations of a simplified version of Modification of Diet in Renal Disease [8], where 0.881 is a coefficient for eGFR specific to the Japanese population [9], $eGFR = 186.3 \times (\text{serum creatinine})^{-1.154} \times (\text{age})^{-0.203} \times 0.881 \times 0.742$ (for female). Individuals were classified as having low eGFR when their eGFR values were <60 ml/min/1.73 m^2 [10]. For the diagnosis of albuminuria, spot urine samples were collected and analyzed; albuminuria was defined to be present when the urinary albumin excretion ratio (UAER), expressed as milligrams as per gram creatinine, was ≥30 mg/g. Normo-, micro-, and macroalbuminuria were defined as an UAER of <30, 30–299, and 300 mg/g or more, respectively. Albuminuria and low eGFR are the components of CKD [10].

Carotid Ultrasonography

Carotid artery status was studied and analyzed as described previously [11]. In brief, carotid artery status was assessed by high-resolution B-mode ultrasonography, using a machine (Sonolayer SSA270A, Toshiba, Japan) equipped with a 7.5-MHz transducer (PLF-703ST, Toshiba). The carotid arteries were examined bilaterally at the levels of the common carotid, the bifurcation, and the internal carotid arteries from transverse and longitudinal orientations by trained sonographers. Carotid intima-media wall thickening was said to occur when the intima-media thickness which was measured at the far wall of the distal 10 mm of the common carotid artery was ≥1.0 mm. Carotid plaque was defined when there is portion that shows the thickness of intima-media complex ≥1.1 mm [12] with the focal protrusion or point(s) of inflexion.

Statistical Analysis

Skewed variables (triglycerides, HOMA-IR, UAER) are presented as median (interquartile range). Other data are expressed as the mean ± SD unless stated otherwise. Analyses of variance, the Mann-Whitney U test, χ^2 tests, and logistic regression analysis were conducted as appropriate to assess the statistical significance of differences between groups using computer software, StatView (Version 5.0; SAS Institute, Cary, N.C., USA) and Dr. SPSS II (Chicago, Ill., USA). A value of $p < 0.05$ was taken to be statistically significant.

Results

Baseline Characteristics

The mean age ± SD of the individuals enrolled was 57.3 ± 11.0 years. Of the 830 individuals examined, 83 (10.0%) had albuminuria, 203 (24.5%) had low eGFR, and 24 (2.9%) had both albuminuria and low eGFR. Therefore, 262 (31.6%) subjects were said to have CKD in our study population. Among 83 who had albuminuria, 75 (9.0%) had microalbuminuria and the remaining 8 (1.0%) had macroalbuminuria. Prevalence of low eGFR in individuals who did not have albuminuria [179/747 (24.0%)] and that in those who had albuminuria [24/83 (28.9%)] did not significantly differ ($p = 0.389$, by the χ^2 test). Individuals with albuminuria had a greater HOMA-IR value than those without CKD (table 1). After adjusting for age and smoking status, logistic regression analysis showed that the odds ratios of albuminuria and low eGFR for increased insulin resistance (defined here as HOMA-IR of ≥2.0) was 4.17 (95% CI 2.22–7.83, $p < 0.001$) and 0.86 (95% CI 0.53–1.40, $p = 0.543$), respectively. When only 630 individuals who had an FPG level of <126 mg/dl and were not taking antidiabetic medication were analyzed, association between albuminuria and increased insulin resistance was still significant with an odds ratio of 2.63 (95% CI 1.49–4.69, $p < 0.001$).

Association between CKD Components and Carotid Plaque

Carotid plaque was more frequently found in individuals with albuminuria than in non-CKD subjects (fig. 1). On the other hand, prevalence of carotid plaque was not significantly different between individuals with low eGFR and those without CKD. Logistic regression analysis showed that, as compared with the no-CKD group, albuminuria was associated with a higher prevalence of carotid plaque after adjusting for age only and after adjustment for age, systolic blood pressure (SBP), FPG, and smoking status (table 2). When HOMA-IR was added as

Table 1. Clinical characteristic and laboratory data in subjects with and without albuminuria and/or low eGFR

	No CKD (n = 568)	CKD (n = 262)	p value	Albuminuria (n = 83)	Low eGFR (n = 203)
Age, years	54.5 ± 10.4	63.4 ± 9.8	<0.001	62.3 ± 11.2	64.1 ± 8.9
Body mass index	21.4 ± 3.0	22.0 ± 3.4	0.016	22.3 ± 4.4	21.8 ± 2.8
Systolic blood pressure, mm Hg	119 ± 19	125 ± 21	<0.001	136 ± 23	122 ± 20
Diastolic blood pressure, mm Hg	74 ± 12	77 ± 13	0.006	82 ± 14	75 ± 12
Antihypertensive medication, n (%)	43 (7.6)	41 (15.6)	<0.001	25 (30.1)	24 (11.8)
Antidiabetic medication, n (%)	4 (0.7)	2 (0.7)	>0.999	1 (1.2)	2 (1.0)
Laboratory data					
Serum calcium, mg/dl	9.3 ± 0.3	9.4 ± 0.3	<0.001	9.4 ± 0.4	9.4 ± 0.3
Serum phosphate, mg/dl	3.7 ± 0.4	3.7 ± 0.4	0.850	3.7 ± 0.4	3.8 ± 0.4
Serum albumin, g/dl	4.5 ± 0.2	4.5 ± 0.2	0.162	4.5 ± 0.2	4.5 ± 0.2
Serum urea nitrogen, mg/dl	13.7 ± 3.3	15.8 ± 4.0	<0.001	15.9 ± 5.4	16.4 ± 4.0
Serum creatinine, mg/dl	0.6 ± 0.1	0.7 ± 0.2	<0.001	0.7 ± 0.3	0.8 ± 0.2
eGFR, ml/min/1.73 m^2	71 ± 8	59 ± 10	<0.001	67 ± 15	55 ± 6
UAER, mg/g	8.0 (5.2–13.1)	11.7 (6.5–37.5)	<0.001	55.8 (39.1–101.2)	8.7 (5.5–15.0)
Uric acid, mg/dl	4.5 ± 0.9	5.1 ± 1.1	<0.001	5.0 ± 1.3	5.2 ± 1.1
Total cholesterol, mg/dl	219 ± 36	230 ± 34	<0.001	227 ± 41	232 ± 32
HDL cholesterol, mg/dl	68 ± 15	67 ± 16	0.841	66 ± 16	68 ± 16
Triglycerides, mg/dl	75 (56–104)	86 (65–119)	<0.001	87 (64–120)	86 (65–119)
Fasting glucose, mg/dl	92 ± 13	96 ± 23	<0.001	105 ± 36	93 ± 11
Hemoglobin A_{1C}, %	5.2 ± 0.5	5.4 ± 0.7	<0.001	5.5 ± 1.0	5.3 ± 0.5
Carotid ultrasonography					
IMT, mm	0.67 ± 0.17	0.75 ± 0.19	<0.001	0.76 ± 0.21	0.75 ± 0.20
max. IMT, mm	1.19 ± 0.54	1.31 ± 0.56	0.003	1.40 ± 0.58	1.27 ± 0.54
Plaque, n (%)	226 (40)	129 (49)	0.013	56 (67)	89 (44)
HOMA-IR	1.04 (0.74–1.47)	1.16 (0.81–1.80)	0.004	1.44 (0.85–2.35)	1.13 (0.81–1.62)
Smoking status					
Never, n (%)	490 (86.3)	234 (89.3)	0.122	71 (85.5)	186 (91.6)
Former, n (%)	34 (6.0)	7 (2.7)		3 (3.6)	5 (2.5)
Current, n (%)	44 (7.7)	21 (8.0)		9 (10.8)	12 (5.9)

Data are means ± SD, median (interquartile range), n, or percentage. UAER indicates the urinary albumin excretion rate. The Mann-Whitney U test was used to evaluate differences in triglycerides, fasting insulin, HOMA-IR, and UAER between no-CKD and CKD groups.

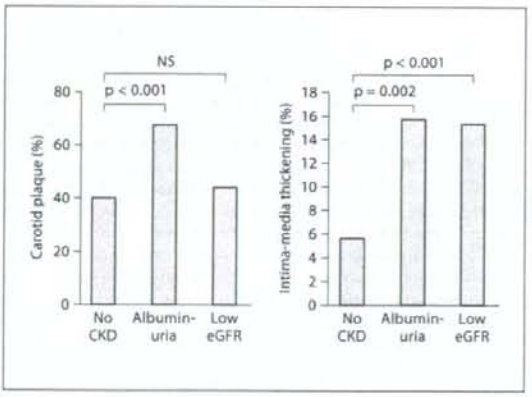

Fig. 1. Prevalence of carotid plaque and carotid artery intima-media thickening and in individuals with or without CKD components.

Table 2. Logistic regression analysis for carotid plaque as a dependent variable

	Odds ratio (95% CI) of albuminuria	p value	Odds ratio (95% CI) of low eGFR	p value
Whole				
Unadjusted	3.11 (1.92–5.03)	<0.001	1.06 (0.77–1.46)	0.723
Adjusted for age	2.48 (1.49–4.11)	<0.001	0.54 (0.37–0.78)	0.001
Adjusted for age, SBP, FPG, and smoking status	2.13 (1.26–3.61)	0.005	0.56 (0.39–0.81)	0.002
Subjects with hypertension (n = 204)				
Unadjusted	1.88 (0.93–3.80)	0.079	0.67 (0.36–1.26)	0.216
Adjusted for age	1.65 (0.80–3.39)	0.173	0.45 (0.22–0.90)	0.025
Adjusted for age, SBP, FPG, and smoking status	1.69 (0.78–3.65)	0.182	0.45 (0.22–0.92)	0.028
Subjects without hypertension (n = 626)				
Unadjusted	3.39 (1.70–6.76)	<0.001	1.23 (0.85–1.78)	0.282
Adjusted for age	3.08 (1.48–6.42)	0.003	0.60 (0.39–0.93)	0.021
Adjusted for age, SBP, FPG, and smoking status	2.83 (1.34–5.96)	0.006	0.61 (0.40–0.95)	0.027
Subjects with high fasting glucose (n = 57)				
Unadjusted	1.36 (0.42–4.39)	0.613	0.87 (0.26–2.96)	0.826
Adjusted for age	1.23 (0.36–4.25)	0.742	0.52 (0.13–2.05)	0.353
Adjusted for age, SBP, and smoking status	1.30 (0.26–6.58)	0.751	0.46 (0.11–1.87)	0.275
Subjects without high fasting glucose (n = 773)				
Unadjusted	3.35 (1.95–5.74)	<0.001	1.08 (0.77–1.50)	0.669
Adjusted for age	2.68 (1.52–4.73)	<0.001	0.55 (0.37–0.80)	0.002
Adjusted for age, SBP, and smoking status	2.39 (1.34–4.24)	0.003	0.57 (0.38–0.82)	0.003

an additional covariate to this statistical mode, albuminuria was still associated with carotid plaque with an odds ratio of 2.12 (95% CI 1.25–3.60, p = 0.005). Positive association between albuminuria and carotid plaque was statistically significant also in individuals without hypertension, defined here as SBP of ≥140 mm Hg, diastolic blood pressure of ≥90 mm Hg or taking antihypertensive medication, and was also statistically significant in those without high fasting glucose, defined here as an FPG level of ≥110 mg/dl or taking antidiabetic medication (table 2). By contrast, low eGFR was associated with a lower prevalence of carotid plaque after adjusting for age or after adjustment for age, SBP, FPG, and smoking status.

Association between CKD Components and Carotid Intima-Media Thickening

Carotid intima-media thickening was more frequently found in individuals with albuminuria or in those with low eGFR than non-CKD subjects (fig. 1). After adjusting for age, association between either of these two CKD components and intima-media thickening lost statistical significance, irrespective of the status of hypertension or high fasting glucose (table 3).

We also analyzed the database which contained 3,318 women who underwent general health screening between 2003 and 2007; not all of them had data of urinary albumin excretion. Age-adjusted logistic regression analysis showed that odds ratio of low eGFR for carotid plaque was 0.67 (95% CI 0.56–0.82, $p < 0.001$) and that for carotid intima-media thickening was 1.11 (95% CI 0.80–1.54, p = 0.54). Therefore, the inverse association between low eGFR and carotid plaque and no significant association between low eGFR and carotid intima-media thickening were observed also in the database containing a female population of larger size.

In addition, after adding the data of men (n = 1,705), we investigated the interaction between gender and CKD components. When carotid plaque was used as a dependent variable, gender showed a significant interaction with both albuminuria and low eGFR ($p < 0.05$). On the other hand, when carotid intima-media thickening was used as a dependent variable, gender showed a significant interaction with albuminuria ($p < 0.05$), but not with low eGFR (p = 0.83).

Serum Levels of Calcium and Phosphorus and Carotid Atherosclerosis in CKD Subjects

We then investigated whether serum levels of calcium and phosphorus were associated with carotid atherosclerosis in individuals with CKD. In individuals with CKD, age-adjusted logistic regression analysis showed that an

Table 3. Logistic regression analysis for carotid intima-media thickening as a dependent variable

	Odds ratio (95% CI) of albuminuria	p value	Odds ratio (95% CI) of low eGFR	p value
Whole				
Unadjusted	2.21 (1.15–4.23)	0.017	2.64 (1.61–4.36)	<0.001
Adjusted for age	1.26 (0.61–2.61)	0.534	1.25 (0.73–2.15)	0.416
Adjusted for age, SBP, FPG, and smoking status	0.74 (0.33–1.66)	0.469	1.34 (0.77–2.33)	0.304
Subjects with hypertension (n = 204)				
Unadjusted	1.28 (0.55–2.97)	0.079	2.68 (1.25–5.74)	0.011
Adjusted for age	0.93 (0.38–2.30)	0.882	1.81 (0.81–4.05)	0.148
Adjusted for age, SBP, FPG, and smoking status	0.89 (0.34–2.32)	0.806	1.82 (0.81–4.11)	0.149
Subjects without hypertension (n = 626)				
Unadjusted	2.04 (0.68–6.11)	0.201	2.70 (1.36–5.35)	0.005
Adjusted for age	1.17 (0.32–4.26)	0.816	1.04 (0.49–2.21)	0.915
Adjusted for age, SBP, FPG, and smoking status	0.69 (0.16–2.97)	0.621	1.09 (0.51–2.36)	0.822
Subjects with high fasting glucose (n = 57)				
Unadjusted	0.53 (0.10–2.82)	0.460	1.40 (0.31–6.36)	0.661
Adjusted for age	0.39 (0.06–2.33)	0.300	0.84 (0.17–4.32)	0.838
Adjusted for age, SBP, and smoking status	0.33 (0.04–2.76)	0.304	0.76 (0.15–3.91)	0.743
Subjects without high fasting glucose (n = 773)				
Unadjusted	2.63 (1.29–5.34)	0.008	2.90 (1.70–4.95)	<0.001
Adjusted for age	1.47 (0.66–3.28)	0.350	1.47 (0.66–3.28)	0.350
Adjusted for age, SBP, and smoking status	1.10 (0.48–2.54)	0.280	1.39 (0.77–2.50)	0.280

odds ratio of serum calcium (per 1 mg/dl increase) was 1.18 (95% CI 0.54–2.57, p = 0.680) for carotid plaque, and 1.51 (95% CI 0.48–4.73, p = 0.477) for carotid intima-media thickening. In these individuals, age-adjusted logistic regression analysis showed that an odds ratio of serum phosphorus (per 1 mg/dl increase) was 0.79 (95% CI 0.42–1.51, p = 0.476) for carotid plaque, and 0.41 (95% CI 0.16–1.06, p = 0.066) for carotid intima-media thickening.

Discussion

In the current study, we have investigated the association between components of CKD (low eGFR and albuminuria) and carotid atherosclerosis in women who underwent general health screening. Univariate analysis showed that albuminuria, but not low eGFR, was significantly positively associated with carotid plaque. The association between albuminuria and carotid plaque remained statistically significant after adjustment for age, SBP, FPG, and smoking status. In addition, positive association between albuminuria and carotid plaque was observed in women without hypertension or in those without high fasting glucose. Although both albuminuria and low eGFR was associated with carotid intima-media thickening by univariate analysis, statistical significance was lost after multivariate adjustment, irrespective of the status of hypertension or high fasting glucose.

Evidence is accumulating that presence of early-phase renal disease may increase the risk of atherosclerotic diseases; however, information over the possible relationship between CKD, especially low eGFR, and carotid artery atherosclerosis seems to be limited. Zhang et al. [6] analyzed the data of 1,264 invited Chinese residents (543 men, 721 women) aged 40 years or older. They found that GFR was negatively associated with carotid intima-media thickness in univariate analysis; however, the observed association lost its statistical significance after adjusting for other atherogenic risk factors. Briet et al. [2] reported that carotid intima-media thickness did not differ significantly between individuals with decreased eGFR and those without. In the previous paper, we reported that low eGFR was associated with carotid intima-media thickening in male individuals when individuals had other atherogenic risk factors, such as hypertension, impaired glucose metabolism, or cigarette smoking [13]. Together with these previous observations, findings in the current study suggested that risk factor properties of low eGFR on carotid atherosclerosis might be different according to the gender. Low eGFR was found to be, although unexpectedly, inversely associated with carotid

plaque in the current study; however, whether there is truly such a relationship or not needs to be further addressed in future studies after increasing the number of enrolled subjects.

Compared to low eGFR, the association of albuminuria with carotid atherosclerosis has more consistently demonstrated by cross-sectional and prospective studies [14–16]. It is possible that impaired glucose/lipid metabolism may represent a mechanism underlying this observed link because albuminuria is known to be associated metabolic syndrome and increased insulin resistance. Consistent with this idea, in the current study, albuminuria was associated with increased insulin resistance (HOMA-IR of $\geq$2.0) with an odds ratio of 4.17. It is of note, however, that association between albuminuria and carotid plaque was found to be independent of SBP, FPG, and HOMA-IR.

It has been reported that serum phosphorus concentration was associated with coronary arterial wall calcification and carotid intima-media thickening in patients with end-stage renal disease [17, 18]. Therefore, here we examined whether serum phosphorus levels were associated with carotid atherosclerosis in individuals with CKD. Serum phosphorus levels were not significantly different between CKD-positive and -negative individuals (table 1). Serum phosphorus levels were found not to be significantly associated with carotid plaque or intima-media thickening by age-adjusted logistic regression analysis, which was in agreement with the observation of Maeda et al. [19]. On the other hand, we previously showed both serum calcium and phosphorus were associated with carotid plaque by analyzing 5,732 subjects [20]. Therefore, the findings in the current study should be re-evaluated after increasing the number of individuals enrolled.

There are several study limitations in the current study. We used the Modification of Diet in Renal Disease formula with the Japanese coefficient of 0.881 for the estimation of GFR [9], which may not be very accurate for values >60 ml/min/1.73 m^2. We could not find a significant association between serum levels of calcium/phosphorus and carotid atherosclerosis in individuals with CKD. It is possible that there may be closer association between these variables when eGFR is much lower. In the current study population, however, only a small fraction of subjects (n = 3) had eGFR level <30 ml/min/1.73 m^2.

In conclusion, by analyzing cross-sectional data from Japanese women who underwent general health screening, we found that albuminuria, but not low eGFR, was positively associated with carotid plaque in univariate analysis. Association between albuminuria and carotid plaque remained statistically significant after multivariate adjustment. It was found to be significant also in individuals without hypertension or in those without high fasting glucose. It may be proposed that, when assessing a possible association between CKD and carotid atherosclerosis, albuminuria and low eGFR should be analyzed separately in women undergoing general health screening, or Ningen Dock.

Acknowledgements

The work was supported in part by a grant from the Smoking Research Foundation, that from Chiyoda Mutual Life Foundation, from the St Luke's Grant for the Epidemiological Research and from Daiwa Securities Health Foundation.

References

1 Go AS, Chertow GM, Fan D, McCulloch CE, Hsu CY: Chronic kidney disease and the risks of death, cardiovascular events, and hospitalization. N Engl J Med 2004;351:1296–1305.

2 Briet M, Bozec E, Laurent S, Fassot C, London GM, Jacquot C, Froissart M, Houillier P, Boutouyrie P: Arterial stiffness and enlargement in mild-to-moderate chronic kidney disease. Kidney Int 2006;69:350–357.

3 Kitamura A, Iso H, Imano H, Ohira T, Okada T, Sato S, Kiyama M, Tanigawa T, Yamagishi K, Shimamoto T: Carotid intima-media thickness and plaque characteristics as a risk factor for stroke in Japanese elderly men. Stroke 2004;35:2788–2794.

4 Rohani M, Jogestrand T, Ekberg M, van der Linden J, Kallner G, Jussila R, Agewall S: Interrelation between the extent of atherosclerosis in the thoracic aorta, carotid intima-media thickness and the extent of coronary artery disease. Atherosclerosis 2005;179:311–316.

5 Brook RD, Bard RL, Patel S, Rubenfire M, Clarke NS, Kazerooni EA, Wakefield TW, Henke PK, Eagle KA: A negative carotid plaque area test is superior to other noninvasive atherosclerosis studies for reducing the likelihood of having underlying significant coronary artery disease. Arterioscler Thromb Vasc Biol 2006;26:656–662.

6 Zhang L, Zhao F, Yang Y, Qi L, Zhang B, Wang F, Wang S, Liu L, Wang H: Association between carotid artery intima-media thickness and early-stage CKD in a Chinese population. Am J Kidney Dis 2007;49:786–792.

7 Leskinen Y, Lehtimaki T, Loimaala A, Lautamatti V, Kallio T, Huhtala H, Salenius JP, Saha H: Carotid atherosclerosis in chronic renal failure – the central role of increased plaque burden. Atherosclerosis 2003;171:295–302.

8 Manjunath G, Sarnak MJ, Levey AS: Prediction equations to estimate glomerular filtration rate: an update. Curr Opin Nephrol Hypertens 2001;10:785–792.

9 Imai E, Horio M: Epidemiology of chronic kidney disease: the difference between Japan and Western countries (in Japanese). J Blood Press 2007;13:359–363.
10 K/DOQI clinical practice guidelines for chronic kidney disease: evaluation, classification, and stratification. Am J Kidney Dis 2002;39:S1–S266.
11 Ishizaka N, Ishizaka Y, Toda E, Nagai R, Yamakado M: Association between serum uric acid, metabolic syndrome, and carotid atherosclerosis in Japanese individuals. Arterioscler Thromb Vasc Biol 2005;25:1038–1044.
12 Handa N, Matsumoto M, Maeda H, Hougaku H, Kamada T: Ischemic stroke events and carotid atherosclerosis. Results of the Osaka Follow-up Study for Ultrasonographic Assessment of Carotid Atherosclerosis (the OSACA Study). Stroke 1995;26:1781–1786.
13 Ishizaka N, Ishizaka Y, Toda E, Koike K, Seki G, Nagai R, Yamakado M: Association between chronic kidney disease and carotid intima-media thickening in individuals with hypertension and impaired glucose metabolism. Hypertens Res 2007;30:1035–1041.
14 Jorgensen L, Jenssen T, Johnsen SH, Mathiesen EB, Heuch I, Joakimsen O, Fosse E, Jacobsen BK: Albuminuria as risk factor for initiation and progression of carotid atherosclerosis in non-diabetic persons: the Tromso Study. Eur Heart J 2007;28:363–369.
15 Ishizaka Y, Ishizaka N, Yamakado M: Albuminuria in general health screening in Japan: relationship with insulin resistance and atherosclerosis. Ningen Dock 2007;21:51–55.
16 Freedman BI, Langefeld CD, Lohman KK, Bowden DW, Carr JJ, Rich SS, Wagenknecht LE: Relationship between albuminuria and cardiovascular disease in type 2 diabetes. J Am Soc Nephrol 2005;16:2156–2161.
17 Goodman WG, Goldin J, Kuizon BD, Yoon C, Gales B, Sider D, Wang Y, Chung J, Emerick A, Greaser L, Elashoff RM, Salusky IB: Coronary-artery calcification in young adults with end-stage renal disease who are undergoing dialysis. N Engl J Med 2000;342:1478–1483.
18 Ishimura E, Taniwaki H, Tabata T, Tsujimoto Y, Jono S, Emoto M, Shoji T, Inaba M, Inoue T, Nishizawa Y: Cross-sectional association of serum phosphate with carotid intima-medial thickness in hemodialysis patients. Am J Kidney Dis 2005;45:859–865.
19 Maeda N, Sawayama Y, Tatsukawa M, Okada K, Furusyo N, Shigematsu M, Kashiwagi S, Hayashi J: Carotid artery lesions and atherosclerotic risk factors in Japanese hemodialysis patients. Atherosclerosis 2003;169:183–192.
20 Ishizaka N, Ishizaka Y, Takahashi E, Tooda E, Hashimoto H, Nagai R, Yamakado M: Serum calcium concentration and carotid artery plaque: a population-based study. J Cardiol 2002;39:151–157.

European Journal of Pharmacology 587 (2008) 237–242

Contents lists available at ScienceDirect

European Journal of Pharmacology

journal homepage: www.elsevier.com/locate/ejphar

Comparison of vasculoprotective effects of benidipine and losartan in a rat model of metabolic syndrome

Gen Matsuzaki [a], Nobukazu Ishizaka [a,*], Kyoko Furuta [a], Makiko Hongo [a], Kan Saito [a], Ryota Sakurai [a], Kazuhiko Koike [b], Ryozo Nagai [a]

[a] Department of Cardiovascular Medicine, University of Tokyo Graduate School of Medicine, Japan
[b] Department of Infectious Diseases, University of Tokyo Graduate School of Medicine, Japan

ARTICLE INFO

Article history:
Received 5 December 2007
Received in revised form 13 March 2008
Accepted 31 March 2008
Available online 9 April 2008

Keywords:
Calcium channel blocker
Angiotensin AT_1 receptor antagonist
Metabolic syndrome
Endothelial dysfunction

ABSTRACT

Although antihypertensive drugs confer improvement in endothelial dysfunction and protection from atherogenesis in hypertension, different classes of antihypertensive drugs may elicit different degrees of vasculoprotective effects. We have investigated the effects of a long-acting calcium antagonist, benidipine, and an angiotensin AT_1 receptor antagonist, losartan, on the vascular damage observed in OLETF rats, an animal model of metabolic syndrome. At 34 weeks of age, OLETF rats were treated with either benidipine (3 mg/kg/day, per os) or losartan (25 mg/kg/day, per os) for 8 weeks. The extent of blood pressure reduction, restoration endothelium-dependent aortic relaxation, and elevation of serum nitrite/nitrate concentration did not differ significantly between benidipine- and losartan-treated OLETF rats. Benidipine and losartan also reduced the aortic expression of transforming growth factor-β1 mRNA and thickening of the vascular wall to a similar extent. Increased cardiac fibrosis was also inhibited by both benidipine and losartan. These data suggest that, when used in an antihypertensive dose, benidipine is as effective as losartan in restoring vascular endothelial function and in suppressing of cardiovascular remodeling in an animal model of metabolic syndrome.

1. Introduction

It has been shown that antihypertensive agents that belong to several different classes are effective in ameliorating endothelial dysfunction, an early feature of vascular damage, in the condition of hypertension (Dohi et al., 1994, Perticone et al., 1999, Taddei et al., 2001, Tschudi et al., 1994, Yao et al., 2003, Zhou et al., 2004). Although controlling blood pressure per se is postulated to largely account for cardiovascular outcome (Wang et al., 2007), blockers of the renin-angiotensin system may be more potent in protecting vascular function in the context of diabetes than other classes of antihypertensive drugs (Cheetham et al., 2000, Cheng et al., 2001, Lindholm et al., 2002, Oniki et al., 2006), including calcium channel blockers (Candido et al., 2004). On the other hand, in the Valsartan Antihypertensive Long-term Use Evaluation (VALUE) trial, it was found that the outcome of cardiac morbidity and mortality did not differ between a treatment group given an angiotensin AT_1 receptor antagonist and one given a calcium channel blocker-based treatment groups in the subgroup of hypertensive patients with diabetes (Zanchetti et al., 2006). This finding supports the concept that intensive control of blood pressure is the most important factor for the reduction of cardiovascular morbidity and mortality even in diabetic patients, regardless of the class of antihypertensive drugs administered (Messerli et al., 2001).

The Otsuka Long-Evans Tokushima Fatty (OLETF) rat is characterized as having increased insulin resistance, diabetes, obesity, hypertension, and dyslipidemia; in other words, metabolic syndrome. In the current study, we aimed to compare the effectiveness of two classes of antihypertensive agents, a long-acting dihydropyridine-calcium channel blocker (benidipine) and an angiotensin AT_1 receptor antagonist (losartan), on the restoration of vascular function and vessel morphology in this rat model of metabolic syndrome.

2. Materials and methods

2.1. Animal models

The experiments were performed in accordance with the guidelines for animal experimentation approved by the Animal Center for Biomedical Research, Faculty of Medicine, University of Tokyo. Male OLETF and age-matched Long-Evans Tokushima Otsuka (LETO) rats were obtained from the Tokushima Research Institute, Otsuka Pharmaceutical (Tokushima, Japan) and maintained under constant temperature and lighting conditions with free access to food and water. At 34 weeks of age, some OLETF rats were given benidipine at a dose of 3 mg/kg/day or losartan at a dose of 25 mg/kg/day per os, which was

* Corresponding author. Department of Cardiovascular Medicine, University of Tokyo Graduate School of Medicine, Hongo 7-3-1 Bunkyo-ku, Tokyo 113-8655, Japan. Tel.: +81 3 3815 5411x37156; fax: +81 3 5842 5586.
E-mail address: nobuishizka-tky@umin.ac.jp (N. Ishizaka).

0014-2999/$ – see front matter © 2008 Elsevier B.V. All rights reserved.
doi:10.1016/j.ejphar.2008.03.061

continued for 8 weeks. One day before the sacrifice, rats were kept in the metabolic cage, and urine was collected for 24 h under fasting condition. Systolic blood pressure and heart rate were measured in conscious rats by tail-cuff plethysmography (BP-98A, Softron, Tokyo, Japan).

2.2. Isolated vascular ring experiments

Ring segments (5 mm in length) of the thoracic aorta were suspended in individual organ chambers filled with Krebs buffer of the following composition (mmol/L): NaCl, 118.3; KCl, 4.7; CaCl2, 2.5; MgSO4, 1.2; KH2PO4, 1.2; NaHCO3, 25.0; and glucose, 10, pH 7.4. The solution was continuously aerated with a 95% O2, 5% CO2 mixture which was maintained at 37°C. Isometric tension was recorded by using an isometric force displacement transducer (NIHON KOHDEN, Tokyo, Japan) connected to a data acquisition system (Power Lab Chart 5, ADInstruments Japan Inc., Nagoya, Japan). The vessels were then precontracted with phenylephrine (3×10^{-6} mol/l). After a stable contraction plateau was reached, the rings were exposed to either acetylcholine or sodium nitroprusside (SNP).

2.3. Real time polymerase chain reaction

Real time reverse transcription polymerase chain reaction (RT-PCR) with gene-specific hybriprobes was performed by LightCycler (Roche Diagnostics, Basel, Switzerland) as described previously (Saito et al., 2005). We examined the three isozymes nitric oxide synthase (NOS). The following primers and probes were used: for transforming growth factor (TGF) -β1: forward 5′ GCAACAACGCAATCTATGAC 3′, reverse 5′ CCTGTATTCCGTCTCCTT 3′ (Nihon Gene Research Lab's Inc., Sendai, Japan); for endothelial NOS (eNOS): forward 5′ CTGGCAAGACCGATTAC-AC 3′, reverse 5′ GTCCAAACACTCCACGCT 3′ (Nihon Gene Research Lab's Inc.); for inducible NOS (iNOS): forward 5′ ACCCAAGGTCTACGTTCAAG 3′, reverse 5′ AAGACCGCACCGAAGATATC 3′ (Nihon Gene Research Lab's Inc.); and for neuronal NOS (nNOS): forward 5′ TGAGCTTTGCGGACAG-GA 3′, reverse 5′ TACGTGAGGCGGAACTTGT 3′. After normalization to the expression of GAPDH mRNA levels, eNOS expression was presented as the percentages of the data from aortas of OLETF rats without benidipine treatment.

2.4. Remodeling of aortic wall and heart

Remodeling of aortic wall was examined as described previously (Ishizaka et al., 2005). Briefly, the paraffin-embedded specimens of thoracic aorta in the 3 μm of thickness were stained with hematoxylin and eosin and Masson's trichrome staining. Vascular wall thickness and perivascular fibrosis were taken as indicators of structural abnormalities of aorta. Quantification of cardiac fibrous areas was performed on the Masson's trichorme stained samples as described previously (Ishizaka et al., 2002). Histopathology and morphometry were performed by investigators who were unaware of the treatment being administered.

2.5. Measurement of serum nitrite/nitrate

After protein-free filtrate of the serum was prepared with the Centricon YM-10 (Millipore, Billerica, MA), concentrations of nitrite/nitrate were measured by the Griess method with the NO2/NO3 Assay Kit-C II (Dojin Chemical Laboratory, Japan). The absorbance of the solution was determined at 540 nm with a micro plate reader, Biotrak II (GE Healthcare, Buckinghamshire, England).

2.6. Statistical analysis

Data are expressed as the mean±S.E.M. We used ANOVA followed by a multiple comparison test to compare raw data, before expressing the results as a percentage of the control value using the statistical analysis software Statistica version 5.1 J for Windows (StatSoft Inc, Tulsa, OK). A value of $P<0.05$ was considered to be statistically significant.

3. Results

3.1. Characteristics of experimental animals

OLETF rats aged 42 weeks were significantly heavier than LETO rats of the same age. Neither antihypertensive agent significantly modified the body weight of OLETF rats (Table 1). Systolic blood pressure was significantly higher in OLETF rats than in LETO rats, and treatment of OLETF rats with either benidipine or losartan lowered blood pressure to a range comparable to that in LETO rats. The plasma fasting glucose level was significantly higher in untreated OLETF rats than in LETO rats, and was affected by neither benidipine nor losartan.

3.2. Relaxations of aortic segments

As compared to the aortas from LETO rats, peak relaxation produced by acetylcholine in the aorta from untreated OLETF rats was significantly reduced, whereas that produced by SNP was not significantly different between LETO and OLETF rats (Fig. 1, Table 2). Both benidipine and losartan reversed, albeit partially, the impaired vascular relaxation in response to acetylcholine in OLETF rats. Neither peak relaxation ($P=0.288$) nor the ED50 ($P=0.128$) in response to acetylcholine was significantly different between the aorta of the OLETF/Ben group and that of the OLETF/Los group.

3.3. Remodeling of aortic wall

As compared to LETO rats, the wall-to-lumen ratio and area of perivascular fibrosis were increased in OLETF rats (Fig. 2). As compared to

Table 1
Characteristics of the experimental animals

Variables	LETO	OLETF	P value (vs. LETO)	OLETF/Ben	P value (vs. OLETF)	OLETF/LOS	P value (vs. OLETF)
n	11	11		11		6	
Body weight (g)	445±8	481±13	0.014	476±11	0.394	470±15	0.311
Systolic blood pressure (mm Hg)	136±2	149±4	0.012	138±3	0.027	135±3	0.015
Heart rate (bpm)	406±21	409±16	0.447	418±15	0.359	408±14	0.482
Heart weight (g)	1.46±0.03	1.85±0.05	<0.001	1.69±0.04	0.010	1.62±0.11	0.049
Heart weight (g/100 g BW)	0.33±0.01	0.40±0.02	0.001	0.36±0.01	0.047	0.34±0.01	0.036
Total cholesterol (mg/dl)	78.7±2.6	78.6±3.0	0.487	79.2±4.5	0.461	78.5±4.3	0.495
Triglyceride (mg/dl)	17.2±2.3	41.0±9.1	0.005	28.5±6.1	0.461	22.8±5.0	0.098
Plasma fasting glucose (mg/dl)	159±4	203±22	0.028	184±16	0.238	187±16	0.288

Values are mean±S.E.M. Both benidipine and losartan lowered the blood pressure of OLETF rats to levels comparable to those of LETO rats. Both hypertensive drugs lowered the heart weight significantly. Levels of serum triglyceride and plasma glucose were also slightly lowered by either antihypertensive drug, although the reduction did not reach statistical significance.

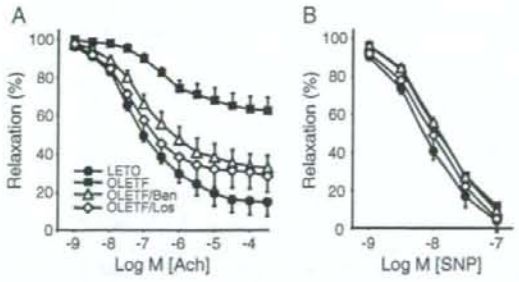

Fig. 1. Endothelium-dependent vascular relaxations in response to acetylcholine (Ach) and endothelium-independent sodium nitroprusside (SNP) in aortic segments from LETO, untreated OLETF, and benidipine and losartan-treated OLETF rats. Vessels were studied as ring segments in organ chambers, and relaxations in response to Ach and SNP were studied after the vessels had been pre-constricted with phenylephrine, 3×10^{-6} mol/l.

LETO rats (100.0±2.9, $n=6$), the luminal area was significantly greater in OLETF rats (138.3±.3, $P<0.001$, $n=6$), OLETF/Ben rats (122.5±5.4, $P<0.001$, $n=6$), and OLETF/Los rats (128.0±5.3, $P<0.001$, $n=6$). Both benidipine and losartan reduced these variables to levels comparable to those in LETO rats. Between the OLETF/Ben and OLETF/Los rats, the difference in the wall-to-lumen ratio ($P=0.336$) and in the area of perivascular fibrosis ($P=0.479$) was not statistically significant. Expression of TGF-β1 mRNA was greater in the aorta of OLETF rats than in that of LETO rats, and both benidipine and losartan reduced the expression of TGF-β1 mRNA in the aorta of OLETF rats (Fig. 3A).

3.4. Serum level of nitrite/nitrate and mRNA expression of NOS isoforms

As compared with the aorta of LETO rats, expression of eNOS and nNOS mRNA was significantly lower, whereas that of iNOS mRNA was significantly higher, in the aorta of OLETF rats (Fig. 3B–D). Both benidipine and losartan reduced the expression eNOS and nNOS mRNA, and increased that of iNOS mRNA, in the aorta of OLETF rats to levels comparable to those in the aorta of LETO rats. The serum nitrite/nitrate level was significantly lower in OLETF rats than in LETO rats; however, it was again increased to a level comparable to that in LETO rats by either benidipine or losartan (Fig. 4).

3.5. Fibrosis of the heart

As compared to the heart of LETO rats, interstitial fibrosis was enhanced in the heart of OLETF rats. Losartan and benidipine suppressed the increase in fibrosis in the heart of OLETF rats to a similar extent (Fig. 5).

4. Discussion

In the current study, we showed that acetylcholine-induced endothelium-dependent vascular relaxation was attenuated in OLETF rats as compared with age-matched LETO rats. Treatment of OLETF rats with an antipressor dose of either losartan or benidipine restored depressed endothelium-dependent vascular relaxation and increased

Table 2
Responses of isolated vessels to acetylcholine and sodium nitroprusside (SNP)

Variables	LETO	OLETF	*P* value (vs. LETO)	OLETF/ Ben	*P* value (vs. OLETF)	OLETF/ LOS	*P* value (vs. OLETF)
n	6	7		7		9	
Ach ED_{50}	7.0±0.3	6.5±0.1	0.037	7.0±0.1	<0.001	7.1±0.2	0.006
Ach peak relaxation	95±4	38±7	<0.001	74±5	0.001	73±7	0.003
SNP ED_{50}	7.6±0.1	7.3±0.1	0.104	7.1±0.0	0.075	7.5±0.2	0.184
SNP peak relaxation	94±8	89±4	0.333	91±2	0.190	95±6	0.169

Values are mean±S.E.M. ED_{50}s are −log[M]. Relaxations are the peak response given as a percentage of the pre-constricted tension. Ach indicates acetylcholine and SNP indicates sodium nitroprusside.

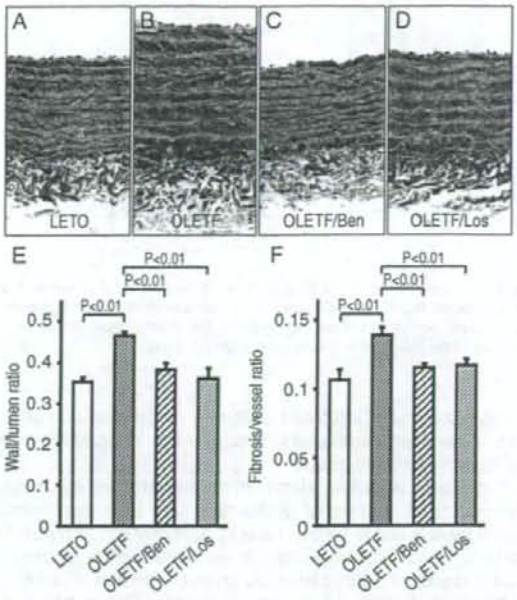

Fig. 2. Effects of benidipine and losartan on vascular remodeling in OLETF rats. (A–D) Masson trichrome staining of the aorta of the LETO rat (A), untreated OLETF rat (B), and benidipine (C) and losartan (D) treated OLETF rat. Both antihypertensive agents significantly reduced the wall/lumen ratio and fibrosis area in the aorta of OLETF rats. Original magnification, ×200. E, F. Values are mean±S.E.M. Summary of the wall-to-lumen ratio (E) and perivascular fibrosis (F) data of the aortas from 4–6 experiments for each group.

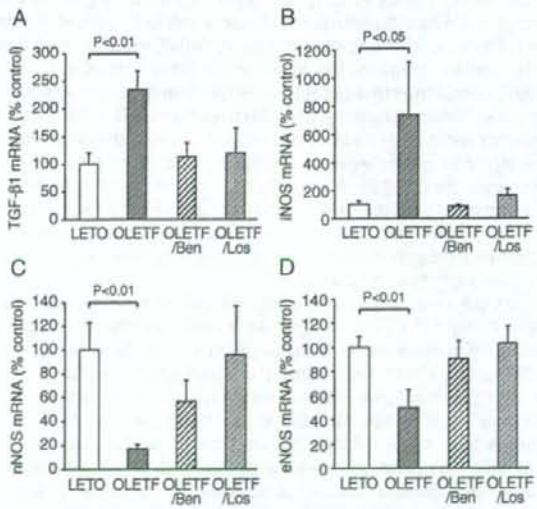

Fig. 3. Effects of benidipine and losartan on mRNA expression of eNOS, iNOS, nNOS, and TGF-β1 Results of quantitative RT-PCR examining the expression of TGF-β1 (A), eNOS (B), iNOS (C), and nNOS (D) mRNA in the aorta of LETO, untreated OLETF, and benidipine and losartan-treated OLETF. Values are mean±S.E.M. Summary of the data from 4–6 experiments for each group.

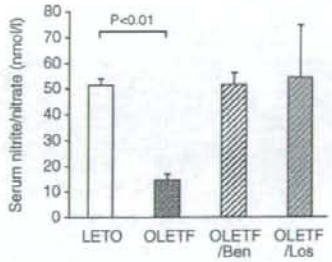

Fig. 4. Effects of benidipine and losartan on serum concentration of nitrite/nitrate in LETO, untreated OLETF, and benidipine and losartan-treated OLETF rats. Serum samples were filtered with a Centricon YM-10 before the assay. Values are mean±S.E.M. Summary of the data from 4–6 experiments for each group.

mRNA expression of eNOS and nNOS to a similar extent. In addition, both of these depressor agents improved aortic and cardiac remodeling, again, to a similar extent.

The effects of various classes of antihypertensive drugs on the preservation of endothelial dysfunction have been investigated in animal models and in human cases of hypertension. Although there might be some differences in the vasculoprotection conferred by various classes of antihypertensive drugs (Bennett et al., 1996), ACE inhibitors, angiotensin AT_1 receptor antagonists (Bennett et al., 1996, Clozel et al., 1990, Dohi et al., 1996), and calcium channel blockers, especially the long-acting ones (Krenek et al., 2001; Tschudi et al., 1994; Wang et al., 2007; Yao et al., 2003; Zhou et al., 2004) are all effective in restoring vascular function in hypertension. In this sense, it is noteworthy that a regiment that based on angiotensin AT_1 receptor antagonist, candesartan and that based on calcium channel blocker, amlodipine, produced no statistical differences in terms of the primary cardiovascular end point in 4728 Japanese hypertensive patients (Ogihara et al., 2008).

In the condition of hypertension with diabetes, however, ACE inhibitors (Baluchnejadmojarad et al., 2004, Oltman et al., 2008) and angiotensin AT_1 receptor antagonists (Cheng et al., 2001; Schafer et al., 2007) may be more effective in cardiovascular protection (Candido et al., 2004). Kagota et al. (2007) reported that an angiotensin AT_1 receptor blocker, telmisartan, but not a calcium channel blocker, amlodipine, ameliorated the impaired endothelium-dependent vasodilatation in spontaneously hypertensive obese rats (Kagota et al., 2007). Considering that certain AT_1 receptor antagonists may potently improve insulin sensitivity, the effectiveness of ACE inhibitors, AT_1 receptor antagonists and calcium channel blockers should further be compared from the viewpoint of cardiovascular protection, as well as renoprotection (Fogari et al., 2007), in the setting of hypertension accompanied with diabetes (Zanchetti et al., 2006) (Kawamori et al., 2006). In addition, an angiotensin AT_1 receptor blocker may be more effective in the prevention of new-onset diabetes than calcium channel blocker (Ogihara et al., 2008).

On the other hand, long-acting calcium channel blockers have been shown to be effective in reducing cardiovascular morbidity and mortality in hypertensive diabetic patients (Tuomilehto et al., 1999). This contrasts with the finding that short-acting, calcium channel blocker treatment may induce a higher rate of cardiovascular events (Borhani et al., 1996; Byington et al., 1998). Several other recent studies have suggested that the outcome of cardiac morbidity and mortality did not differ between angiotensin AT_1 receptor antagonist-based and calcium channel blocker-based treatment groups in patients with both diabetes and hypertension (Zanchetti et al., 2006), supporting the idea that blood pressure control is most important for the reduction of cardiovascular morbidity and mortality in diabetic hypertensive patients regardless of the classes of antihypertensive drugs (Messerli et al., 2001). Therefore, the finding that benidipine and losartan showed similar efficacy in restoring vascular function and cardiovascular morphology in the current study would seem to be in agreement with this idea. On the other hand, as we did not compare the subdepressor dose of antihypertensive drugs, we could not conclude that there may not be a difference in the vasculoprotective effects between the two classes of antihypertensive agents tested when used at a subdepressor dose or in combination with other drugs.

What is the mechanism underlying the preferable effects of benidipine and losartan in the current study? Many studies have shown that eNOS plays a crucial role in vasculoprotection (Forstermann and Munzel, 2006). In the current study, expression of eNOS and nNOS was found to be significantly lower in OLETF rats than in LETO rats; however, both benidipine and losartan preserved eNOS/nNOS expression and increased the serum nitrite/nitrate concentrations. It has also been reported that angiotensin AT_1 receptor antagonist (Yamamoto et al., 2007) and long-acting calcium channel blockers (Ding and Vaziri, 2000; Kobayashi et al., 1999; Toba et al., 2005) can upregulate vascular eNOS expression in hypertension. It has been reported that nNOS is also expressed in vascular cells, especially in certain pathological conditions, such as atherosclerosis and hypertension (Boulanger et al., 1998; Kishi et al., 2003), and nNOS, like eNOS, may also exert important vasculoprotective actions against vascular lesion formation (Channon et al., 1998). It has been reported that ACE inhibitors and angiotensin AT_1 receptor antagonists increase nNOS expression in the adrenal glands (Qadri et al., 2001). In addition, it has been proposed that iNOS induction may be involved in the pathophysiological process leading to inflammation, endothelial dysfunction, and atherosclerosis (Nagareddy et al., 2005, Vane et al., 1994). Therefore, benidipine- and losartan-mediated reduction of iNOS expression, which is enhanced in the aorta of OLETF rats, may be a preferable phenomenon in terms of vasculoprotection. Reduction of iNOS expression might be independent of the antipressor effects of benidipine or losartan, because it has been reported that calcium channel blockers and angiotensin AT_1 receptor antagonists may reduce iNOS expression in cultured cells (Chou et al., 2002, Neri Serneri et al., 2004). This point should be examined in future studies. We also showed that benidipine reduced the cardiac fibrosis in the heart of OLETF rats at 42 weeks of age. This finding is in agreement with a previous report that benidipine is also effective in inhibiting the cardiac remodeling, seen in the pressure-overload model (Liao et al., 2005) and in OELTF rats (Jesmin et al., 2006).

In conclusion, we showed here that, when used in an antihypertensive dose, a long-acting calcium channel blocker, benidipine and an angiotensin AT_1 receptor antagonist, losartan, were equally effective in restoring vascular function and in suppressing cardiovascular remodeling in an animal model of metabolic syndrome. The mechanisms

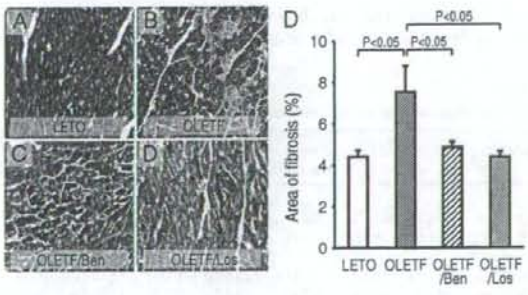

Fig. 5. Effects of benidipine and losartan on cardiac fibrosis. (A–D) Representative image of Masson trichrome staining of the heart of the LETO (A), untreated OLETF (B), and benidipine (C) and losartan (D) treated OLETF rats. (D) Values are mean±S.E.M. Summary of the fibrosis area data from 4–6 experiments for each group.

underlying these preferable effects may include upregulation of vascular expression of eNOS and nNOS, and downregulation of fibrosis-related genes, such as TGF-β1.

Acknowledgements

This work was supported by Grants in Aid for Scientific Research from the Ministry of Education, Science, and Culture of Japan (Grant 19590937) and Grant from the Takeda Science Foundation, the Sankyo Foundation of Life Science, and Okinaka Memorial Institute for Medical Research.

References

Baluchnejadmojarad, T., Roghani, M., Imani, A., 2004. Dose-dependent effect of captopril on aortic reactivity of streptozotocin-diabetic rats. Clin. Exp. Pharmacol. Physiol. 31, 342–347.

Bennett, M.A., Hillier, C., Thurston, H., 1996. Endothelium-dependent relaxation in resistance arteries from spontaneously hypertensive rats: effect of long-term treatment with perindopril, quinapril, hydralazine or amlodipine. J. Hypertens. 14, 389–397.

Borhani, N.O., Mercuri, M., Borhani, P.A., Buckalew, V.M., Canossa-Terris, M., Carr, A.A., Kappagoda, T., Rocco, M.V., Schnaper, H.W., Sowers, J.R., Bond, M.G., 1996. Final outcome results of the Multicenter Isradipine Diuretic Atherosclerosis Study (MIDAS). A randomized controlled trial. JAMA 276, 785–791.

Boulanger, C.M., Heymes, C., Benessiano, J., Geske, R.S., Levy, B.I., Vanhoutte, P.M., 1998. Neuronal nitric oxide synthase is expressed in rat vascular smooth muscle cells: activation by angiotensin II in hypertension. Circ. Res. 83, 1271–1278.

Byington, R.P., Furberg, C.D., Craven, T.E., Pahor, M., Sowers, J.R., 1998. Isradipine in prediabetic hypertensive subjects. Diabetes Care 21, 2103–2110.

Candido, R., Allen, T.J., Lassila, M., Cao, Z., Thallas, V., Cooper, M.E., Jandeleit-Dahm, K.A., 2004. Irbesartan but not amlodipine suppresses diabetes-associated atherosclerosis. Circulation 109, 1536–1542.

Channon, K.M., Qian, H., Neplioueva, V., Blazing, M.A., Olmez, E., Shetty, G.A., Youngblood, S.A., Pawloski, J., McMahon, T., Stamler, J.S., George, S.E., 1998. In vivo gene transfer of nitric oxide synthase enhances vasomotor function in carotid arteries from normal and cholesterol-fed rabbits. Circulation 98, 1905–1911.

Cheetham, C., Collis, J., O'Driscoll, G., Stanton, K., Taylor, R., Green, D., 2000. Losartan, an angiotensin type 1 receptor antagonist, improves endothelial function in non-insulin-dependent diabetes. J. Am. Coll. Cardiol. 36, 1461–1466.

Cheng, Z.J., Vaskonen, T., Tikkanen, I., Nurminen, K., Ruskoaho, H., Vapaatalo, H., Muller, D., Park, J.K., Luft, F.C., Mervaala, E.M., 2001. Endothelial dysfunction and salt-sensitive hypertension in spontaneously diabetic Goto-Kakizaki rats. Hypertension 37, 433–439.

Chou, T.C., Yang, S.P., Pei, D., 2002. Amlodipine inhibits pro-inflammatory cytokines and free radical production and inducible nitric oxide synthase expression in lipopolysaccharide/interferon-gamma-stimulated cultured vascular smooth muscle cells. Jpn. J. Pharmacol. 89, 157–163.

Clozel, M., Kuhn, H., Hefti, F., 1990. Effects of angiotensin converting enzyme inhibitors and of hydralazine on endothelial function in hypertensive rats. Hypertension 16, 532–540.

Ding, Y., Vaziri, N.D., 2000. Nifedipine and diltiazem but not verapamil up-regulate endothelial nitric-oxide synthase expression. J. Pharmacol. Exp. Ther. 292, 606–609.

Dohi, Y., Criscione, L., Pfeiffer, K., Luscher, T.F., 1994. Angiotensin blockade or calcium antagonists improve endothelial dysfunction in hypertension: studies in perfused mesenteric resistance arteries. J. Cardiovasc. Pharmacol. 24, 372–379.

Dohi, Y., Kojima, M., Sato, K., 1996. Benidipine improves endothelial function in renal resistance arteries of hypertensive rats. Hypertension 28, 58–63.

Fogari, R., Derosa, G., Zoppi, A., Preti, P., Lazzari, P., Destro, M., Fogari, E., Rinaldi, A., Mugellini, A., 2007. Effect of telmisartan-amlodipine combination at different doses on urinary albumin excretion in hypertensive diabetic patients with microalbuminuria. Am. J. Hypertens. 20, 417–422.

Forstermann, U., Munzel, T., 2006. Endothelial nitric oxide synthase in vascular disease: from marvel to menace. Circulation 113, 1708–1714.

Ishizaka, N., Saito, K., Mitani, H., Yamazaki, I., Sata, M., Usui, S., Mori, I., Ohno, M., Nagai, R., 2002. Iron overload augments angiotensin II-induced cardiac fibrosis and promotes neointima formation. Circulation 106, 1840–1846.

Ishizaka, N., Saito, K., Mori, I., Matsuzaki, G., Ohno, M., Nagai, R., 2005. Iron chelation suppresses ferritin upregulation and attenuates vascular dysfunction in the aorta of angiotensin II-infused rats. Arterioscler. Thromb. Vasc. Biol. 25, 2282–2288.

Jesmin, S., Hattori, Y., Maeda, S., Zaedi, S., Sakuma, I., Miyauchi, T., 2006. Subdepressor dose of benidipine ameliorates diabetic cardiac remodeling accompanied by normalization of upregulated endothelin system in rats. Am. J. Physiol, Heart Circ. Physiol. 290, H2146–H2154.

Kagota, S., Tada, Y., Kubota, Y., Nejime, N., Yamaguchi, Y., Nakamura, K., Kunitomo, M., Shinozuka, K., 2007. Peroxynitrite is involved in the dysfunction of vasorelaxation in SHR/NDmcr-cp rats, spontaneously hypertensive obese rats. J. Cardiovasc. Pharmacol. 50, 677–685.

Kawamori, R., Daida, H., Tanaka, Y., Miyauchi, K., Kitagawa, A., Hayashi, D., Kishimoto, J., Ikeda, S., Imai, Y., Yamazaki, T., 2006. Amlodipine versus angiotensin II receptor blocker; control of blood pressure evaluation trial in diabetics (ADVANCED-J). BMC Cardiovasc. Disord. 6, 39.

Kishi, T., Hirooka, Y., Mukai, Y., Shimokawa, H., Takeshita, A., 2003. Atorvastatin causes depressor and sympatho-inhibitory effects with upregulation of nitric oxide synthases in stroke-prone spontaneously hypertensive rats. J. Hypertens. 21, 379–386.

Kobayashi, N., Kobayashi, K., Hara, K., Higashi, T., Yanaka, H., Yagi, S., Matsuoka, H., 1999. Benidipine stimulates nitric oxide synthase and improves coronary circulation in hypertensive rats. Am. J. Hypertens. 12, 483–491.

Krenek, P., Salomone, S., Kyselovic, J., Wibo, M., Morel, N., Godfraind, T., 2001. Lacidipine prevents endothelial dysfunction in salt-loaded stroke-prone hypertensive rats. Hypertension 37, 1124–1128.

Liao, Y., Asakura, M., Takashima, S., Ogai, A., Asano, Y., Asanuma, H., Minamino, T., Tomoike, H., Hori, M., Kitakaze, M., 2005. Benidipine, a long-acting calcium channel blocker, inhibits cardiac remodeling in pressure-overloaded mice. Cardiovasc. Res. 65, 879–888.

Lindholm, L.H., Ibsen, H., Dahlof, B., Devereux, R.B., Beevers, G., de Faire, U., Fyhrquist, F., Julius, S., Kjeldsen, S.E., Kristiansson, K., Lederballe-Pedersen, O., Nieminen, M.S., Omvik, P., Oparil, S., Wedel, H., Aurup, P., Edelman, J., Snapinn, S., 2002. Cardiovascular morbidity and mortality in patients with diabetes in the Losartan Intervention For Endpoint reduction in hypertension study (LIFE): a randomised trial against atenolol. Lancet 359, 1004–1010.

Messerli, F.H., Grossman, E., Goldbourt, U., 2001. Antihypertensive therapy in diabetic hypertensive patients. Am. J. Hypertens. 14, 12S–16S.

Nagareddy, P.R., Xia, Z., McNeill, J.H., MacLeod, K.M., 2005. Increased expression of iNOS is associated with endothelial dysfunction and impaired pressor responsiveness in streptozotocin-induced diabetes. Am. J. Physiol, Heart Circ. Physiol. 289, H2144–H2152.

Neri Serneri, G.G., Boddi, M., Modesti, P.A., Coppo, M., Cecioni, I., Toscano, T., Papa, M.L., Bandinelli, M., Lisi, G.F., Chiavarelli, M., 2004. Cardiac angiotensin II participates in coronary microvessel inflammation of unstable angina and strengthens the immunomediated component. Circ. Res. 94, 1630–1637.

Ogihara, T., Nakao, K., Fukui, T., Fukiyama, K., Ueshima, K., Oba, K., Sato, T., Saruta, T., 2008. Effects of candesartan compared with amlodipine in hypertensive patients with high cardiovascular risks: candesartan antihypertensive survival evaluation in Japan trial. Hypertension 51, 393–398.

Oltman, C.L., Davidson, E.P., Coppey, L.J., Kleinschmidt, T.L., Lund, D.D., Adebara, E.T., Yorek, M.A., 2008. Vascular and neural dysfunction in Zucker diabetic fatty rats: a difficult condition to reverse. Diabetes Obes. Metab. 10, 64–74.

Oniki, H., Fujii, K., Kansui, Y., Goto, K., Iida, M., 2006. Effects of angiotensin II receptor antagonist on impaired endothelium-dependent and endothelium-independent relaxations in type II diabetic rats. J. Hypertens. 24, 331–338.

Perticone, F., Ceravolo, R., Maio, R., Ventura, G., Iacopino, S., Cuda, G., Mastroroberto, P., Chello, M., Mattioli, P.L., 1999. Calcium antagonist isradipine improves abnormal endothelium-dependent vasodilation in never treated hypertensive patients. Cardiovasc. Res. 41, 299–306.

Qadri, F., Arens, T., Schwartz, E.C., Hauser, W., Dominiak, P., 2001. Angiotensin-converting enzyme inhibitors and AT1-receptor antagonist restore nitric oxide synthase (NOS) activity and neuronal NOS expression in the adrenal glands of spontaneously hypertensive rats. Jpn. J. Pharmacol. 85, 365–369.

Saito, K., Ishizaka, N., Hara, M., Matsuzaki, G., Sata, M., Mori, I., Ohno, M., Nagai, R., 2005. Lipid accumulation and transforming growth factor-beta upregulation in the kidneys of rats administered angiotensin II. Hypertension 46, 1180–1185.

Schafer, A., Flierl, U., Vogt, C., Menninger, S., Tas, P., Ertl, G., Bauersachs, J., 2007. Telmisartan improves vascular function and reduces platelet activation in rats with streptozotocin-induced diabetes mellitus. Pharmacol. Res. 56, 217–223.

Taddei, S., Virdis, A., Ghiadoni, L., Magagna, A., Pasini, A.F., Garbin, U., Cominacini, L., Salvetti, A., 2001. Effect of calcium antagonist or beta blockade treatment on nitric oxide-dependent vasodilation and oxidative stress in essential hypertensive patients. J. Hypertens. 19, 1379–1386.

Toba, H., Nakagawa, Y., Miki, S., Shimizu, T., Yoshimura, A., Inoue, R., Asayama, J., Kobara, M., Nakata, T., 2005. Calcium channel blockades exhibit anti-inflammatory and antioxidative effects by augmentation of endothelial nitric oxide synthase and the inhibition of angiotensin converting enzyme in the N(G)-nitro-L-arginine methyl ester-induced hypertensive rat aorta: vasoprotective effects beyond the blood pressure-lowering effects of amlodipine and manidipine. Hypertens. Res. 28, 689–700.

Tschudi, M.R., Criscione, L., Novosel, D., Pfeiffer, K., Luscher, T.F., 1994. Antihypertensive therapy augments endothelium-dependent relaxations in coronary arteries of spontaneously hypertensive rats. Circulation 89, 2212–2218.

Tuomilehto, J., Rastenyte, D., Birkenhager, W.H., Thijs, L., Antikainen, R., Bulpitt, C.J., Fletcher, A.E., Forette, F., Goldhaber, A., Palatini, P., Sarti, C., Fagard, R., 1999. Effects of calcium-channel blockade in older patients with diabetes and systolic hypertension. Systolic Hypertension in Europe Trial Investigators. N. Engl. J. Med. 340, 677–684.

Vane, J.R., Mitchell, J.A., Appleton, I., Tomlinson, A., Bishop-Bailey, D., Croxtall, J., Willoughby, D.A., 1994. Inducible isoforms of cyclooxygenase and nitric-oxide synthase in inflammation. Proc. Natl. Acad. Sci. U. S. A. 91, 2046–2050.

Wang, J.G., Li, Y., Franklin, S.S., Safar, M., 2007. Prevention of stroke and myocardial infarction by amlodipine and angiotensin receptor blockers: a quantitative overview. Hypertension 50, 181–188.

Yamamoto, E., Yamashita, T., Tanaka, T., Kataoka, K., Tokutomi, Y., Lai, Z.F., Dong, Y.F., Matsuba, S., Ogawa, H., Kim-Mitsuyama, S., 2007. Pravastatin enhances beneficial effects of olmesartan on vascular injury of salt-sensitive hypertensive rats, via pleiotropic effects. Arterioscler. Thromb. Vasc. Biol. 27, 556–563.

Yao, K., Sato, H., Sonoda, R., Ina, Y., Suzuki, K., Ohno, T., 2003. Effects of benidipine and candesartan on kidney and vascular function in hypertensive Dahl rats. Hypertens. Res. 26, 569–576.

Zanchetti, A., Julius, S., Kjeldsen, S., McInnes, G.T., Hua, T., Weber, M., Laragh, J.H., Plat, F., Battegay, E., Calvo-Vargas, C., Cieslinski, A., Degaute, J.P., Holwerda, N.J., Kobalava, J., Pedersen, O.L., Rudyatmoko, F.P., Siamopoulos, K.C., Storset, O., 2006. Outcomes in subgroups of hypertensive patients treated with regimens based on valsartan and amlodipine: an analysis of findings from the VALUE trial. J. Hypertens. 24, 2163–2168.

Zhou, M.S., Jaimes, E.A., Raij, L., 2004. Inhibition of oxidative stress and improvement of endothelial function by amlodipine in angiotensin II-infused rats. Am. J. Hypertens. 17, 167–171.

European Journal of Pharmacology 604 (2009) 87–92

Contents lists available at ScienceDirect

European Journal of Pharmacology

journal homepage: www.elsevier.com/locate/ejphar

Cardiovascular Pharmacology

Administration of angiotensin II, but not catecholamines, induces accumulation of lipids in the rat heart

Makiko Hongo [a], Nobukazu Ishizaka [a,*], Kyoko Furuta [a], Naoya Yahagi [b], Kan Saito [a], Ryota Sakurai [a], Gen Matsuzaki [a], Kazuhiko Koike [c], Ryozo Nagai [a]

[a] Department of Cardiovascular Medicine, University of Tokyo, Graduate School of Medicine, Hongo 7-3-1, Bunkyo-ku, Tokyo 113-8655, Japan
[b] Department of Diabetes and Metabolic Disease, University of Tokyo, Graduate School of Medicine, Hongo 7-3-1, Bunkyo-ku, Tokyo 113-8655, Japan
[c] Department of Infectious Disease, University of Tokyo, Graduate School of Medicine, Hongo 7-3-1, Bunkyo-ku, Tokyo 113-8655, Japan

ARTICLE INFO

Article history:
Received 9 May 2008
Received in revised form 20 November 2008
Accepted 3 December 2008
Available online 10 December 2008

Keywords:
Angiotensin II
Lipid accumulation
Lipotoxicity
Gene expression

ABSTRACT

Accumulation of lipids in the heart may cause cardiac dysfunction in various disorders, such as obesity and diabetes. In the current study, we have investigated whether administration of angiotensin II or norepinephrine induces accumulation of lipids and/or changes in the expression of genes related to lipid metabolism in the rat heart. Lipid deposition was found in myocardial, vascular wall, and perivascular cells of the angiotensin II-infused rat heart, and superoxide generation was increased in these lipid-positive cells. By contrast, intracardiac lipid deposition was not found in the heart of norepinephrine-induced hypertensive rats. Triglyceride content in the heart tissue of angiotensin II-infused rats increased more than 3-fold as compared with untreated controls. Losartan completely, but hydralazine only partially, suppressed the angiotensin II-induced intracardiac lipid deposition and increase in tissue triglyceride content. Administration of angiotensin II upregulated the mRNA expression of sterol regulatory element-binding protein-1c and fatty acid synthase, but downregulated that of uncoupling protein 2 and 3, in a manner dependent on the angiotensin AT_1 receptor. Collectively, these results suggest that angiotensin II may be involved in modulating both intracardiac lipid content and lipid metabolism-related gene expression, in part via an angiotensin AT_1 receptor-dependent and pressor-independent mechanism.

1. Introduction

Accumulation of lipids in non-adipose tissues can occur in certain disease conditions, including aging, over-nutrition, obesity, and diabetes, and may play a crucial role in the pathogenesis of tissue damage (Schaffer, 2003), a phenomenon referred to as lipotoxicity (Unger, 2002). Inappropriate accumulation of free fatty acids and neutral lipids can also be observed in the myocardium; this accumulation may result in both functional and morphological damage, such as systolic and/or diastolic dysfunction of the left ventricle (Chiu et al., 2005, Zhou et al., 2000), ventricular wall hypertrophy (Finck et al., 2003, Horiuchi et al., 1993), and interstitial fibrosis (Lee et al., 2004). In previous studies, we found that administration of angiotensin II to rats causes deposition of lipids in tubular epithelial and vascular wall cells in the kidney (Ishizaka et al., 2006, Saito et al., 2005), where cellular proliferation may be promoted. In the current study, we have investigated whether administration of two different pressor agents, angiotensin II and a catecholamine, causes intracardiac accumulation of lipids, and modulates the expression of genes related to lipid metabolism.

2. Materials and methods

2.1. Animal models

The experiments were performed in accordance with the guidelines for animal experimentation approved by the Animal Center for Biomedical Research, Faculty of Medicine, University of Tokyo. Angiotensin II-induced hypertension was induced in male Sprague-Dawley rats (250 to 300 g) by subcutaneous implantation of an osmotic minipump (Alza Pharmaceutical) as described previously (Ishizaka et al., 1997). Briefly, Val^5-angiotensin II (Sigma Chemical) was infused at doses of 0.7 mg/kg/day. Norepinephrine (Sigma Chemical) was infused at a dose of 2.8 mg/kg/day for 7 days using the same system. In some angiotensin II-infused rats, angiotensin AT_1 receptor antagonist, losartan (25 mg/kg/day), or the nonspecific vasodilator, hydralazine (15 mg/kg/day) (Sigma Chemical), both of which normalized the blood pressure of angiotensin II-infused rats, was given in the drinking water (Ishizaka et al., 2002).

* Corresponding author. Department of Cardiovascular Medicine, University of Tokyo, Graduate School of Medicine, Hongo 7-3-1, Bunkyo-ku, Tokyo 113-8655, Japan. Tel.: +81 3 3815 5411x3016; fax: +81 3 3974 2236.
E-mail address: noburishizka-tky@umin.ac.jp (N. Ishizaka).

0014-2999/$ – see front matter © 2009 Elsevier B.V. All rights reserved.
doi:10.1016/j.ejphar.2008.12.006

Table 1
Oligonucleotide primers used in this study

Gene	GenBank no.	Forward primer	Reverse primer
PPAR-α	NM_013196	GTGGCTGCTATAATTTGCTG	TGAAGGAGTTTTGGGAAGAG
PPAR-γ	NM_013124	ATCAGCTCTGTGGACCTCTC	AGGCTCTACTTTGATCGCAC
SREBP-1c	XM_213329	CTGATGGAGACAGGGAGTTC	ATCACCACGGCTGTCAGT
FAS	M76767	CTGGAACGTGAACATGATCT	TTCACCAGCAGGATACTCAG
HMG-CoA reductase	NM_013134	GACACTTACAATCTGTATGATG	CTTGGAGAGGTAAAACTGCCA
CPT-1	NM_031559	ATCGACCGCCATCTCTTC	CTCAAAGTCAAAGAGCTCCAC
CPT-2	NM_012930	TGACCAAAGAAGCAGCGAT	TTGTGGTTCATCTGCTGGTA
DGAT-1	NM_053437	TCTTCCTACCGGGATGTCAATC	TCCCTGCAGACACAGCTTTG
PGC-1α	AY237127	TCATTACCTACCGTTACACCT	CATACTTGCTCTTGGTGGAA
UCP2	BC062230	TGGTCGGAGATACCAGAG	GTCTGTCATGAGGTTGGCT
UCP3	AF035973	GTCCGATTTCAAGCCATGAT	CTTGTGATGTTGGGCCAAGT
Nox1	MN_053683	TGGACGAATTAGGCAAACCG	TTGGGGTGGGCAGTAGCTAT
Nox4	AY027527	AACACTGGTGAAGATTTGC	CTGAGGGATGATTGATTACTG
GAPDH	NM_017008	TGAACGGGAAGCTCACTGG	TCCACCACCCTGTTGCTGTA

PPAR, peroxisome proliferator-activated receptor; SREBP, sterol regulatory element-binding protein; FAS, fatty acid synthase; HMG-CoAR, 3-hydroxy-3-methylglutaryl coenzyme A reductase; CPT, carnitine palmitoyltransferase; DGAT, diacylglycerol acyltransferase; PGC, PPAR-γ coactivator; UCP, uncoupling protein; and GAPDH, glyceraldehyde-3-phosphate dehydrogenase.

2.2. Measurement of lipid contents in the serum and the heart

Serum levels of total cholesterol, triglycerides, and nonesterified fatty acid were measured by enzymatic methods (SRL). Contents of triglycerides, total cholesterol, and free cholesterol in the heart tissue were measured from homogenate extracts by enzymatic colorimetric determination using Triglyceride-E Test, Cholesterol-E Test, and Free cholesterol-E Test Wako, respectively (Wako Pure Chemicals).

2.3. Histological analysis

Oil red O staining was performed on sections of unfixed, freshly frozen heart samples (3 μm in thickness). The areas of lipid deposition were calculated by using the image analysis software, Photoshop (Adobe), and semiquantification of the lipid deposition was performed as described elsewhere (Ishizaka et al., 2006). Staining with the oxidative fluorescent dye dihydroethidium (DHE) was performed as described previously (Saito et al., 2004). Images were obtained with a fluorescent microscope BX51 (Olympus), and the fluorescence intensity, obtained from at least five fields for each section, was presented as the percentage of that of untreated control.

2.4. Western blot analysis

Western blot analysis was performed as described previously (Aizawa et al., 2000). Antibodies against total and phosphorylated forms AMP-activated protein kinase (Cell Signaling), sterol regulatory element-binding protein (SREBP)-1 (Santa Cruz Biotechnology), SREBP-2 (Santa Cruz Biotechnology), ATP-binding cassette transporter subfamily A1 (ABCA1) (Novus Biologicals), scavenger receptor class B type 1 (SR-B1) (Novus Biologicals), and mitochondrial superoxide dismutase (mt SOD) (Upstate) were used at a dilution of 1/1000.

2.5. Real time reverse transcription-polymerase chain reaction (RT-PCR)

Expression of lipid metabolism-related gene mRNA was analyzed by real time quantitative PCR performed by LightCycler together with hybriprobe technology (Roche Diagnostics). Expression of target genes was normalized to the mRNA expression of endogenous control, glyceraldehyde-3-phosphate dehydrogenase (GAPDH). The target genes were as follows: peroxisome proliferator-activated receptor (PPAR)-α (Nihon Gene Research Lab's Inc., Sendai, Japan), PPAR-γ, SREBP-1c, fatty acid synthase (FAS), 3-hydroxy-3-methylglutaryl coenzyme A reductase (HMG-CoAR), carnitine palmitoyltransferase (CPT)-1, CPT-2, diacylglycerol acyltransferase (DGAT)-1, PPAR-γ coactivator (PGC)-1α, uncoupling protein (UCP)2, UCP3, Nox1, and Nox4. The forward and backward primers used are described in Table 1.

2.6. Statistical analysis

Data are expressed as the mean ± S. E. M. We used ANOVA followed by a multiple comparison test to compare raw data, before expressing the results as a percentage of the control value using the statistical analysis software StatView ver. 5.0 (SAS Institute). A value of $P<0.05$ was considered to be statistically significant.

3. Results

3.1. Characteristics of experimental animals

The hemodynamic parameters in each group have been reported elsewhere (Aizawa et al., 2000). Angiotensin II and norepinephrine elevated the blood pressure to a similar extent, and both hydralazine and losartan completely suppressed the blood pressure elevation induced by angiotensin II. Angiotensin II, but not norepinephrine, significantly increased the serum levels of triglycerides and non-esterified fatty acids, and these increases were inhibited by losartan, but not by hydralazine (Fig. 1A–C).

3.2. Tissue contents of lipids

The tissue content of triglycerides, total cholesterol, and free cholesterol was found to be increased in the heart of angiotensin II-

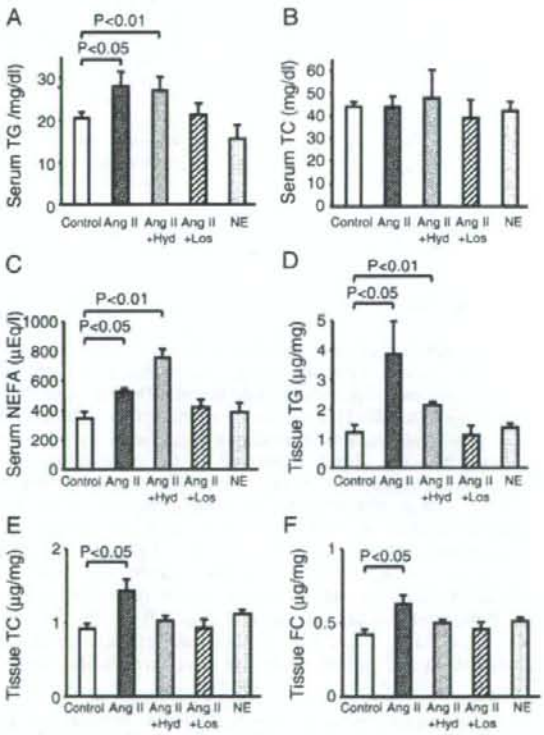

Fig. 1. Serum levels and tissue content of lipids. A–C. Serum levels of triglycerides (TG) (A), total cholesterol (TC) (B), and non-esterified fatty acids (NEFA) (C). D–E. Content of triglycerides (D), total cholesterol (E), free cholesterol (FC) (F) in the heart tissue. Shown in a summary of data from 4–6 rats in each group. Ang II, angiotensin II; Hyd, hydralazine; Los, losartan; and NE, norepinephrine.

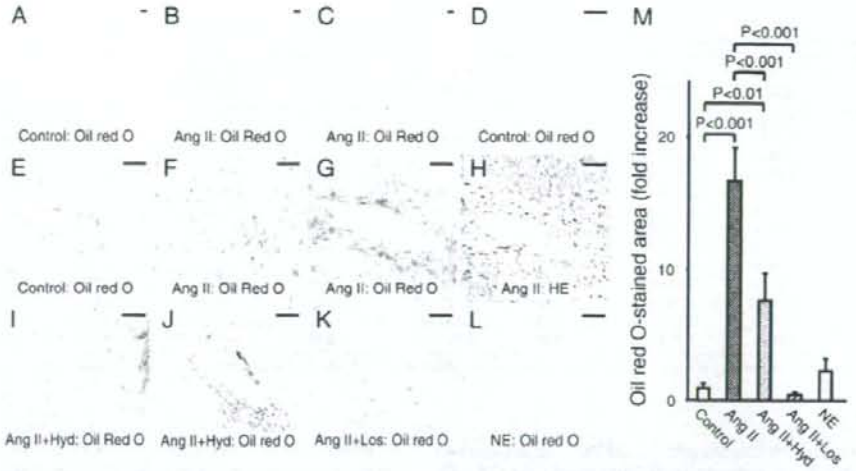

Fig. 2. Accumulation of lipids in the heart. A, D, E. Heart section from a control rat. B, C, F–H. Heart sections from angiotensin II (Ang II)-infused rats. I, J. Heart section from a rat given both angiotensin II and hydralazine (Hyd). K. Heart section from a rat given both angiotensin II and losartan (Los). L. Heart section from a rat given norepinephrine (NE). F and G are serial sections. A–G, I–L. Oil red O staining. H. Hematoxylin eosin (HE) staining. Lipid droplets were not observed in the myocardium or vascular regions (A, D, E) of control rats. Lipid droplets were present in both the myocardium (B, C, F) and perivascular regions (G) in the heart of angiotensin II-infused rats. Lipid droplets in the myocardium (I) and perivascular regions (J) were observed in the heart of rats given both angiotensin II and hydralazine, but not in the heart of rats given angiotensin II plus losartan (K) or those given norepinephrine (L). Original magnification, ×100 (A–C), and ×200 (D–L). Scale bars indicate 50 μm. M. Semiquantification of the oil red O-stained area. Shown is a summary of data from 5–7 experiments in each group.

infused rats, but not norepinephrine-infused rats (Fig. 1). Hydralazine only partially suppressed the angiotensin II-induced increase in intracardiac triglyceride content, but it completely suppressed the increase in intracardiac total cholesterol and free cholesterol content (Fig. 1D–F). Losartan suppressed the angiotensin II-induced increase in all three lipid fractions tested. Administration of losartan alone or hydralazine alone did not significantly alter the lipid content of the heart (losartan: triglycerides, 1.53±0.12 μg/mg, $n=4$; total cholesterol, 1.16±0.07 μg/mg, $n=3$; free cholesterol, 0.53±0.04 μg/mg, $n=4$; hydralazine: triglycerides, 1.40±0.14 μg/mg, $n=4$; total cholesterol, 1.09±0.14 μg/mg, $n=4$; free cholesterol, 0.43±0.04 μg/mg, $n=5$).

3.3. Staining for lipids

Oil red O staining of heart sections showed no apparent lipid deposition in the heart of untreated rats (Fig. 2A, D, E). By contrast, accumulation of oil red O-stainable lipid was observed in the myocardium as well as the arterial wall of angiotensin II-infused rats (Fig. 2B, C, F, G). In the angiotensin II-infused rat heart, lipid accumulation was also observed in perivascular regions, especially where remodeling of perivascular regions was apparent (Fig. 2G, H), and in granulation regions (data not shown). Lipid deposition remained present in the heart when angiotensin II-infused rats were concomitantly treated with hydralazine (Fig. 2I, J). On the other hand, lipid deposition was not apparent, or was very minor when present, in heart sections from rats treated with both angiotensin II and losartan or from rats treated with norepinephrine infusion (Fig. 2K, L). Semiquantitative measurements of the oil red O-stained areas are summarized in Fig. 2M.

3.4. Co-localization of lipid deposition and superoxide

As compared with untreated controls, DHE staining-positive signals were increased in the heart of angiotensin II-infused rats, and

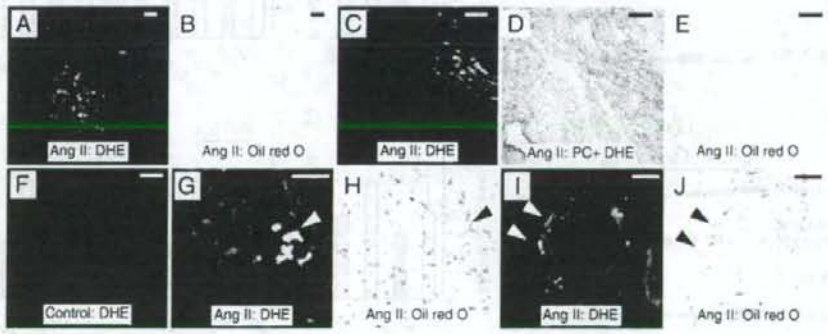

Fig. 3. Lipid and superoxide staining of the heart section. A–E, F–J. Heart sections from angiotensin (Ang) II-infused rats. F. Heart section from a control rat. A, C, F, G, I Dihydroethidium (DHE) staining. D. Phase contrast (PC) microscopic image overlaid with DHE staining image. B, E, H, J. Oil red O staining. C and D are the same section. C (=D)–E, G–H, and I–J are serial sections. Some cells with intense DHE staining (arrowheads in G and I) contained lipid deposits (arrowheads in H and J). Original magnification, ×100 (A–C), ×200 (C–H), and ×400 (I, J). Scale bars indicate 50 μm.

Table 2
mRNA levels of genes related to lipid metabolism

Gene	Control (n=6)	Ang II (n=6)	P	Ang II+Hyd (n=5)	P	Ang II+Los (n=6)	P	NE (n=7)	P
PPAR-α	1±0.17	1.88±0.34	0.030	2.99±0.64	0.005	1.41±0.20	0.080	2.00±0.18	0.001
PPAR-γ	1±0.17	3.30±0.98	0.019	4.25±1.13	0.032	0.83±0.09	0.19	3.56±0.44	<0.001
SREBP-1c	1±0.24	3.66±1.02	0.008	2.67±0.96	0.039	0.71±0.12	0.14	0.77±0.17	0.21
FAS	1±0.17	2.97±0.32	<0.001	3.46±1.00	<0.001	1.30±0.17	0.18	1.28±0.13	0.18
HMG-CoA reductase	1±0.20	2.29±0.30	<0.001	2.50±0.66	0.009	0.99±0.23	0.49	0.98±0.33	0.48
CPT-1	1±0.06	0.55±0.09	<0.001	1.08±0.29	0.395	0.82±0.15	0.154	0.16±0.03	<0.001
CPT-2	1±0.04	0.63±0.06	<0.001	0.67±0.10	<0.001	0.66±0.06	<0.001	0.67±0.05	<0.001
DGAT-1	1±0.04	1.20±0.12	0.071	0.58±0.18	0.003	0.60±0.04	<0.001	0.87±0.12	0.14
PGC-1α	1±0.09	0.52±0.06	<0.001	0.59±0.18	<0.005	0.94±0.18	0.395	1.34±0.31	0.17
UCP2	1±0.08	0.51±0.08	<0.001	0.39±0.08	<0.001	0.80±0.09	0.055	1.53±0.79	0.276
UCP3	1±0.06	0.75±0.09	0.020	0.50±0.11	<0.001	0.74±0.14	0.037	2.10±0.49	0.038
Nox1	1±0.21	3.31±0.61	0.006	4.87±1.82	0.026	0.90±0.19	0.378	1.17±0.42	0.367
Nox4	1±0.21	5.25±2.22	0.047	0.72±0.10	0.093	1.17±0.12	0.199	1.17±0.14	0.206

P values are versus untreated control. Ang II, angiotensin II; Hyd, hydralazine; Los, losartan; and NE, norepinephrine. Other abbreviations were same as Table 1.

semiquantitative measurements showed that the DHE-stained area was significantly greater after angiotensin II infusion (control 100±37%, $n=5$, versus angiotensin II 342±125%, $n=5$; $P<0.05$). In the heart of angiotensin II-infused rats, some myocardial cells that had increased superoxide staining were found to be positive for lipid deposition (lower magnification in Fig. 3A, B, and higher magnification in Fig. 3C–D). Similarly, some vascular wall and perivascular cells with increased superoxide staining were found to contain lipid deposits (Fig. 3G–J).

3.5. Regulation of genes related to lipid metabolism

Next, we examined the expression of lipid metabolism-related genes after infusion of the pressor agents (Table 2). mRNA expression of PPAR-α, PPAR-γ, SREBP-1c, FAS, and HMG-CoAR was found to be increased in the heart of rats that received angiotensin II infusion. Of the genes tested, mRNA expression of PPAR-α and PPAR-γ was also increased in the heart of the norepinephrine-infused rat. The expression of PGC-1α, UCP2 and UCP3 was decreased after angiotensin II infusion, but not after norepinephrine infusion. The angiotensin II-induced regulation of these genes (PPAR-α, PPAR-γ, SREBP-1c, FAS, HMG-CoAR, PGC-1α, UCP2, and UCP3) was suppressed by losartan, but not by hydralazine. On the other hand, mRNA expression of CPT-1 and CPT-2 was downregulated by angiotensin II. We found that the angiotensin II-induced CPT-1 downregulation was suppressed by depressor agents, and that norepinephrine also downregulated CPT-1 mRNA expression; therefore, the angiotensin II-induced CPT-1 mRNA downregulation might be induced by hypertension per se. Angiotensin II increased the mRNA expression of two components of NAD(P)H oxidase, Nox1 and Nox4.

Angiotensin II did not alter the protein expression of AMPKα; however, it increased the levels of phosphorylated AMPKα, and this increase was inhibited by either depressor agent (Fig. 4). Protein expression of matured SREBP-1 was increased by angiotensin II, and this increase was suppressed by losartan, but not by hydralazine.

We also examined the expression of several other lipid metabolism-related proteins. In the heart of control ($n=4$) and angiotensin II-

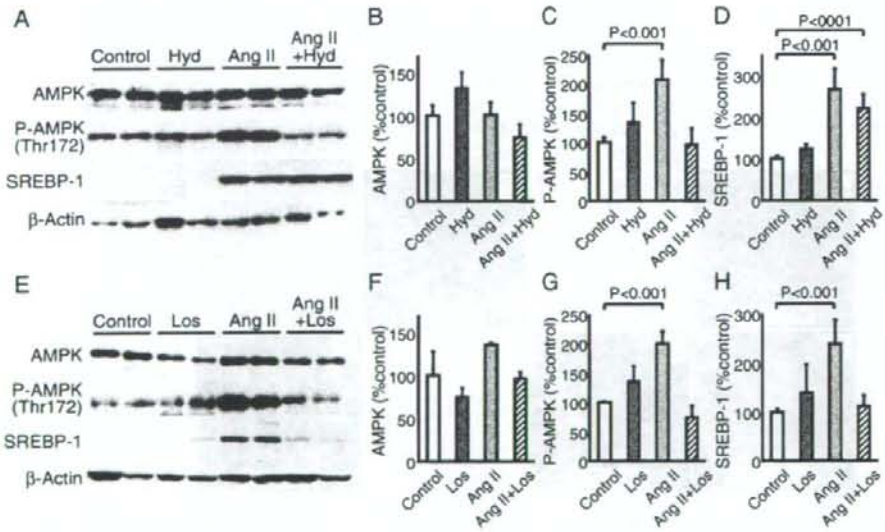

Fig. 4. Western blot analysis of AMP-activated protein kinase (AMPK), phosphorylated (activated) form of AMPKα (P-AMPK), and SREPB-1. A, E. Representative blots. B–D, F–H. Summary of data from 4–6 experiments in each group. Abbreviations are same as Table 1.

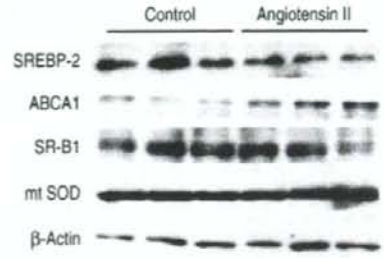

Fig. 5. Western blot analysis of proteins related to lipid metabolism. Shown are the results of the expression in the heart of control and angiotensin II-infused rats of the following proteins: Sterol regulatory element-binding protein (SREBP)-2, ATP-binding cassette transporter subfamily A-1 (ABCA1), scavenger receptor class B type 1 (SR-B1), mitochondrial superoxide dismutase (mt SOD).

infused ($n=4$) rats, the expression of these proteins was, respectively (% control): SREBP-2: 100±17 versus 78±14 (P=NS); ABCA1: 100±10 versus 172±7 ($P<0.001$); SR-B1: 100±17 versus 127±18 (P=NS); mit SOD: 100±5 versus 110±18 (P=NS) (Fig. 5).

4. Discussion

In the present study, we showed that administration of angiotensin II, but not catecholamines, caused accumulation of lipids in myocardial, vascular wall, and perivascular cells in the rat heart. Such angiotensin II-induced lipid deposition, as well as the increases in tissue triglyceride content in the heart, was suppressed completely by losartan, but only partially by hydralazine. These findings collectively indicate that the accumulation of intracardiac lipids induced by angiotensin II was, at least in part, independent of the pressor properties of angiotensin II.

Intracardiac lipid accumulation, which is sometimes designated 'cardiac steatosis' (McGavock et al., 2007), is known to occur in humans in certain diseased conditions, such as diabetes and heart failure (McGavock et al., 2007, Sharma et al., 2004). By means of genetic engineering, several animal models showing an amount of intracardiac lipids have been generated; these models include mice with cardiac-specific overexpression of acyl CoA synthase (Lee et al., 2004), fatty acid transport protein 1(Chiu et al., 2005), and PPAR-α (Finck et al., 2003), and mice with cardiac-restricted deletion of PPAR-delta (Cheng et al., 2004). The observation that accumulation of excessive fatty acids aggravates, whereas reduction of cardiac lipid content ameliorates, the structural and functional damage in these models supports the notion that accumulation of excessive lipid may indeed be cardiotoxic. In our previous studies, we found that administration of angiotensin II, but not catecholamines, caused marked accumulation of neutral lipids in the kidney (Ishizaka et al., 2006, Saito et al., 2005), leading us to investigate whether these two pressor agents affect cardiac lipid content differently in the current study.

What would be the mechanism underlying angiotensin II-induced intracardiac lipid deposition? We found that angiotensin II upregulated the expression of SREBP-1c, FAS, and HMG-CoAR, and downregulated that of UCP2, and UCP3; in addition, the pattern of regulation paralleled intracardiac lipid accumulation. It has been reported that angiotensin II upregulates the expression of SREBP-1c and FAS, resulting in increased lipogenesis in adipocytes in vitro (Jones et al., 1997, Kim et al., 2001). In addition, although the physiological functions of UCP2 and UCP3 are not well-established, downregulation of these new UCPs may augment the production of reactive oxygen species and decrease the catalysis of transported fatty acids (Affourtit et al., 2007). We also found that angiotensin II upregulated PPAR-α mRNA expression. Overexpression of PPAR-α in the heart may also cause lipotoxic cardiomyopathy (Finck et al., 2003, Vikramadithyan et al., 2005), suggesting that PPAR-α upregulation might be an underlying mechanism linking angiotensin II administration and cardiac lipid deposition.

Several previous studies have shown that PPAR-α activator may ameliorate myocardial damage induced by angiotensin II (Fujita et al., 2008, Ichihara et al., 2006). In the current study, we also found that PPAR-α expression was increased by norepinephrine infusion, which did not cause apparent cardiac lipid accumulation, indicating that upregulation of cardiac PPAR-α may not solely account for lipid accumulation in the heart. Whether or not PPAR-α activator acts to enhance or to suppress angiotensin II-induced lipid accumulation in the heart should be examined in future studies.

Activation of AMPK may result in the phosphorylation of acetyl CoA carboxylase, followed by the reduction of malonyl CoA and the subsequent activation and upregulation of CPT-1, leading to the stimulation of fatty acid oxidation (Affourtit et al., 2007). In the current study, we found that angiotensin II activated cardiac AMPK; however, it downregulated CPT-1 mRNA expression. Tian et al. (2001) have recently reported that pressure overload-induced cardiac hypertrophy causes a significant increase in AMPK activity in the heart that is, unexpectedly, accompanied by a downregulation of CPT-1 expression. They presumed that, unlike short-term activation, prolonged activation of AMPK might result in a downregulation of the enzymes that would be critical to fatty acid oxidation. With regard to this, it may be of note that, in the current study, both AMPK activation and CPT-1 downregulation by angiotensin II were suppressed not only by losartan, but also by hydralazine, and that CPT-1 mRNA downregulation was also induced by norepinephrine-induced hypertension, suggesting that these events were induced not in an angiotensin II-specific manner, but rather by hypertension itself.

It has been reported that UCP2 may reduce the generation of ROS, and conversely, downregulation of uncoupling proteins may increase the generation of ROS (Arsenijevic et al., 2000). On the other hand, enhanced oxidative stress or increased amounts of ROS may activate or upregulate SREBP-1 and FAS (Furuta et al., 2008, Gharavi et al., 2006). In addition, CuZn-SOD deficiency has been reported to increase lipid accumulation in the liver (Uchiyama et al., 2006). We found in our previous study (Saito et al., 2005) and the current one that superoxide is histologically co-localized with lipid deposition in the heart and kidney of angiotensin II-infused rats. Taken together, these findings may collectively suggest that angiotensin II-induced deposition of lipid in the heart may be evoked, at least in part, by enhanced oxidative stress (Fig. 5). This hypothesis should be examined in future studies (Fig. 6).

In conclusion, administration of angiotensin II to rats induced intracardiac lipid accumulation in regions where superoxide

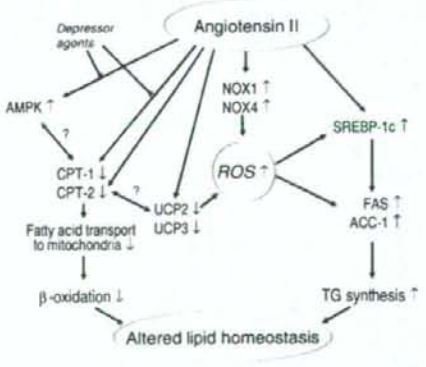

Fig. 6. Working hypothesis on angiotensin II-induced altered lipid homeostasis. Abbreviations are same as in Table 1. ROS indicates reactive oxygen species.

production was found to be increased. The angiotensin II-induced accumulation of intracardiac lipids, in addition to regulation of the expression of several lipid metabolism-related genes (SREBP-1c, FAS, HMG-CoAR, PGC-1α, UCP2, and UCP3), events that were not mimicked by catecholamine infusion, were found to be dependent on the angiotensin AT_1 receptor. The physiological significance of angiotensin II-induced cardiac lipid accumulation and the role of enhanced oxidative stress on this phenomenon await further investigation.

Acknowledgements

This work was supported by Grants in Aid for Scientific Research from the Ministry of Education, Science, and Culture of Japan (Grant 19590937) and Grant from the Takeda Science Foundation, the Sankyo Foundation of Life Science, Okinaka Memorial Institute for Medical Research, and Daiwa Securities Health Foundation.

References

Affourtit, C., Crichton, P.G., Parker, N., Brand, M.D., 2007. Novel uncoupling proteins. Novartis Found. Symp. 287, 70–80 Discussion 80–91.
Aizawa, T., Ishizaka, N., Taguchi, J., Nagai, R., Mori, I., Tang, S.S., Ingelfinger, J.R., Ohno, M., 2000. Heme oxygenase-1 is upregulated in the kidney of angiotensin II-induced hypertensive rats: possible role in renoprotection. Hypertension 35, 800–806.
Arsenijevic, D., Onuma, H., Pecqueur, C., Raimbault, S., Manning, B.S., Miroux, B., Couplan, E., Alves-Guerra, M.C., Goubern, M., Surwit, R., Bouillaud, F., Richard, D., Collins, S., Ricquier, D., 2000. Disruption of the uncoupling protein-2 gene in mice reveals a role in immunity and reactive oxygen species production. Nat. Genet. 26, 435–439.
Cheng, L., Ding, G., Qin, Q., Huang, Y., Lewis, W., He, N., Evans, R.M., Schneider, M.D., Brako, F.A., Xiao, Y., Chen, Y.E., Yang, Q., 2004. Cardiomyocyte-restricted peroxisome proliferator-activated receptor-delta deletion perturbs myocardial fatty acid oxidation and leads to cardiomyopathy. Nat. Med. 10, 1245–1250.
Chiu, H.C., Kovacs, A., Blanton, R.M., Han, X., Courtois, M., Weinheimer, C.J., Yamada, K.A., Brunet, S., Xu, H., Nerbonne, J.M., Welch, M.J., Fettig, N.M., Sharp, T.L., Sambandam, N., Olson, K.M., Ory, D.S., Schaffer, J.E., 2005. Transgenic expression of fatty acid transport protein 1 in the heart causes lipotoxic cardiomyopathy. Circ. Res. 96, 225–233.
Finck, B.N., Han, X., Courtois, M., Aimond, F., Nerbonne, J.M., Kovacs, A., Gross, R.W., Kelly, D.P., 2003. A critical role for PPARalpha-mediated lipotoxicity in the pathogenesis of diabetic cardiomyopathy: modulation by dietary fat content. Proc. Natl. Acad. Sci. U. S. A. 100, 1226–1231.
Fujita, K., Maeda, N., Sonoda, M., Ohashi, K., Hibuse, T., Nishizawa, H., Nishida, M., Hiuge, A., Kurata, A., Kihara, S., Shimomura, I., Funahashi, T., 2008. Adiponectin protects against angiotensin II-induced cardiac fibrosis through activation of PPAR-alpha. Arterioscler. Thromb. Vasc. Biol. 28, 863–870.
Furuta, E., Pai, S.K., Zhan, R., Bandyopadhyay, S., Watabe, M., Mo, Y.Y., Hirota, S., Hosobe, S., Tsukada, T., Miura, K., Kamada, S., Saito, K., Iiizumi, M., Liu, W., Ericsson, J., Watabe, K., 2008. Fatty acid synthase gene is up-regulated by hypoxia via activation of Akt and sterol regulatory element binding protein-1. Cancer Res. 68, 1003–1011.
Gharavi, N.M., Baker, N.A., Mouillesseaux, K.P., Yeung, W., Honda, H.M., Hsieh, X., Yeh, M., Smart, E.J., Berliner, J.A., 2006. Role of endothelial nitric oxide synthase in the regulation of SREBP activation by oxidized phospholipids. Circ. Res. 98, 768–776.
Horiuchi, M., Yoshida, H., Kobayashi, K., Kuriwaki, K., Yoshimine, K., Tomomura, M., Koizumi, T., Nikaido, H., Hayakawa, J., Kuwajima, M., et al., 1993. Cardiac hypertrophy in juvenile visceral steatosis (jvs) mice with systemic carnitine deficiency. FEBS Lett. 326, 267–271.
Ichihara, S., Obata, K., Yamada, Y., Nagata, K., Noda, A., Ichihara, G., Yamada, A., Kato, T., Izawa, H., Murohara, T., Yokota, M., 2006. Attenuation of cardiac dysfunction by a PPAR-alpha agonist is associated with down-regulation of redox-regulated transcription factors. J. Mol. Cell. Cardiol. 41, 318–329.
Ishizaka, N., de Leon, H., Laursen, J.B., Fukui, T., Wilcox, J.N., De Keulenaer, G., Griendling, K.K., Alexander, R.W., 1997. Angiotensin II-induced hypertension increases heme oxygenase-1 expression in rat aorta. Circulation 96, 1923–1929.
Ishizaka, N., Aizawa, T., Yamazaki, I., Usui, S., Mori, I., Kurokawa, K., Tang, S.S., Ingelfinger, J.R., Ohno, M., Nagai, R., 2002. Abnormal iron deposition in renal cells in the rat with chronic angiotensin II administration. Lab. Invest. 82, 87–96.
Ishizaka, N., Matsuzaki, G., Saito, K., Noiri, E., Mori, I., Nagai, R., 2006. Expression and localization of PDGF-B, PDGF-D, and PDGF receptor in the kidney of angiotensin II-infused rat. Lab. Invest. 86, 1285–1292.
Jones, B.H., Standridge, M.K., Moustaid, N., 1997. Angiotensin II increases lipogenesis in 3T3-L1 and human adipose cells. Endocrinology 138, 1512–1519.
Kim, S., Dugail, I., Standridge, M., Claycombe, K., Chun, J., Moustaid-Moussa, N., 2001. Angiotensin II-responsive element is the insulin-responsive element in the adipocyte fatty acid synthase gene: role of adipocyte determination and differentiation factor 1/sterol-regulatory-element-binding protein 1c. Biochem. J. 357, 899–904.
Lee, Y., Naseem, R.H., Duplomb, L., Park, B.H., Garry, D.J., Richardson, J.A., Schaffer, J.E., Unger, R.H., 2004. Hyperleptinemia prevents lipotoxic cardiomyopathy in acyl CoA synthase transgenic mice. Proc. Natl. Acad. Sci. U. S. A. 101, 13624–13629.
McGavock, J.M., Lingvay, I., Zib, I., Tillery, T., Salas, N., Unger, R., Levine, B.D., Raskin, P., Victor, R.G., Szczepaniak, L.S., 2007. Cardiac steatosis in diabetes mellitus: a 1H-magnetic resonance spectroscopy study. Circulation 116, 1170–1175.
Saito, K., Ishizaka, N., Aizawa, T., Sata, M., Iso, O.N., Noiri, E., Ohno, M., Nagai, R., 2004. Role of aberrant iron homeostasis in the upregulation of transforming growth factor-beta1 in the kidney of angiotensin II-induced hypertensive rats. Hypertens. Res. 27, 599–607.
Saito, K., Ishizaka, N., Hara, M., Matsuzaki, G., Sata, M., Mori, I., Ohno, M., Nagai, R., 2005. Lipid accumulation and transforming growth factor-beta upregulation in the kidneys of rats administered angiotensin II. Hypertension 46, 1180–1185.
Schaffer, J.E., 2003. Lipotoxicity: when tissues overeat. Curr. Opin. Lipidol. 14, 281–287.
Sharma, S., Adrogue, J.V., Golfman, L., Uray, I., Lemm, J., Youker, K., Noon, G.P., Frazier, O.H., Taegtmeyer, H., 2004. Intramyocardial lipid accumulation in the failing human heart resembles the lipotoxic rat heart. Faseb. J. 18, 1692–1700.
Tian, R., Musi, N., D'Agostino, J., Hirshman, M.F., Goodyear, L.J., 2001. Increased adenosine monophosphate-activated protein kinase activity in rat hearts with pressure-overload hypertrophy. Circulation 104, 1664–1669.
Uchiyama, S., Shimizu, T., Shirasawa, T., 2006. Cu/Zn-SOD deficiency causes ApoB degradation and induces hepatic lipid accumulation by impaired lipoprotein secretion in mice. J. Biol. Chem. 281, 31713–31719.
Unger, R.H., 2002. Lipotoxic diseases. Annu. Rev. Med. 53, 319–336.
Vikramadithyan, R.K., Hirata, K., Yagyu, H., Hu, Y., Augustus, A., Homma, S., Goldberg, I.J., 2005. Peroxisome proliferator-activated receptor agonists modulate heart function in transgenic mice with lipotoxic cardiomyopathy. J. Pharmacol. Exp. Ther. 313, 586–593.
Zhou, Y.T., Grayburn, P., Karim, A., Shimabukuro, M., Higa, M., Baetens, D., Orci, L., Unger, R.H., 2000. Lipotoxic heart disease in obese rats: implications for human obesity. Proc. Natl. Acad. Sci. U. S. A. 97, 1784–1789.

JOURNAL OF VIROLOGY, Sept. 2008, p. 8349–8361
0022-538X/08/$08.00+0 doi:10.1128/JVI.00306-08

Vol. 82, No. 17

Intramembrane Processing by Signal Peptide Peptidase Regulates the Membrane Localization of Hepatitis C Virus Core Protein and Viral Propagation▽

Kiyoko Okamoto,[1]† Yoshio Mori,[1]† Yasumasa Komoda,[1] Toru Okamoto,[1] Masayasu Okochi,[2] Masatoshi Takeda,[2] Tetsuro Suzuki,[3] Kohji Moriishi,[1] and Yoshiharu Matsuura[1]*

Department of Molecular Virology, Research Institute for Microbial Diseases,[1] and Department of Post-Genomics and Diseases, Division of Psychiatry and Behavioral Proteomics, Graduate School of Medicine,[2] Osaka University, Osaka, and Department of Virology II, National Institute of Infectious Diseases, Tokyo,[3] Japan

Received 12 February 2008/Accepted 11 June 2008

Hepatitis C virus (HCV) core protein has shown to be localized in the detergent-resistant membrane (DRM), which is distinct from the classical raft fraction including caveolin, although the biological significance of the DRM localization of the core protein has not been determined. The HCV core protein is cleaved off from a precursor polyprotein at the lumen side of Ala[191] by signal peptidase and is then further processed by signal peptide peptidase (SPP) within the transmembrane region. In this study, we examined the role of SPP in the localization of the HCV core protein in the DRM and in viral propagation. The C terminus of the HCV core protein cleaved by SPP in 293T cells was identified as Phe[177] by mass spectrometry. Mutations introduced into two residues (Ile[176] and Phe[177]) upstream of the cleavage site of the core protein abrogated processing by SPP and localization in the DRM fraction. Expression of a dominant-negative SPP or treatment with an SPP inhibitor, L685,458, resulted in reductions in the levels of processed core protein localized in the DRM fraction. The production of HCV RNA in cells persistently infected with strain JFH-1 was impaired by treatment with the SPP inhibitor. Furthermore, mutant JFH-1 viruses bearing SPP-resistant mutations in the core protein failed to propagate in a permissive cell line. These results suggest that intramembrane processing of HCV core protein by SPP is required for the localization of the HCV core protein in the DRM and for viral propagation.

The hepatitis C virus (HCV), which has infected an estimated 170 million people worldwide, leads to chronic hepatitis, which in turn causes severe liver diseases, including steatosis, cirrhosis, and eventually hepatocellular carcinoma (47). HCV possesses a positive-sense single-stranded RNA with a nucleotide length of 9.6 kb, which encodes a single large precursor polyprotein composed of about 3,000 amino acids. The viral polyprotein is processed by cellular and viral proteases into structural and nonstructural proteins (24). The development of efficient therapies for hepatitis C had been hampered by the lack of a reliable cell culture system, as well as by the absence of a small-animal model. Lohmann et al. established an HCV replicon, which consisted of an antibiotic selection marker and a genotype 1b HCV RNA, and showed that it replicated autonomously in the intracellular compartments of a human hepatoma cell line, Huh7 (16). The replicon system has been used as an important tool in the investigation of HCV replication, and it has served as a cell-based assay system for the evaluation of antiviral compounds. Recently, cell culture systems for in vitro replication and infectious-virus production were established based on the full-length HCV genome of a genotype 2a isolate, which was recovered from a fulminant hepatitis C patient (15, 45, 50). However, the molecular mechanism of the HCV life cycle in host cells has not been well characterized.

Several viruses have been reported to utilize a lipid raft composed of cholesterol and sphingolipids upon entry (34). The lipid raft is characterized by resistance to nonionic detergents at 4°C and includes caveolin, glycolipids, and other substances (40). Several nonenveloped viruses enter cells through a caveola/raft-mediated endosome, designated the caveosome, and then translocate to the endoplasmic reticulum (ER), endosome, or nucleus (34, 35), although enveloped viruses generally enter host cells through a clathrin-dependent pathway (18). HCV is enclosed by a host cell-derived membrane and belongs to the family *Flaviviridae*. Several reports suggest that HCV enters host cells through general endocytosis, such as by a clathrin-mediated pathway (5, 6, 22). However, HCV has been suggested to replicate on a detergent-resistant membrane (DRM), including some characteristic membrane structures such as lipid rafts and membranous webs (8, 9, 38). In a previous report, an HCV replication complex prepared from a cell fraction treated with a nonionic detergent was shown to be enzymatically active (2). HCV nonstructural proteins remodel the intracellular membrane to form a replication complex that includes several host proteins (8, 46). The HCV core protein has a C-terminal transmembrane region that is anchored on intracellular compartments such as the ER and mitochondria and on the surfaces of lipid droplets (10, 30, 42). Recent studies have indicated that assembly of HCV particles occurs around lipid droplets that are surrounded by the remodeled membranes (23). Although the HCV core protein functions as a capsid protein, it is found in the DRM fraction, which is

* Corresponding author. Mailing address: Department of Molecular Virology, Research Institute for Microbial Diseases, Osaka University, 3-1 Yamada-oka, Suita, Osaka 565-0871, Japan. Phone: 81-6-6879-8340. Fax: 81-6-6879-8269. E-mail: matsuura@biken.osaka-u.ac.jp.
† K. Okamoto and Y. Mori contributed equally to this work.
▽ Published ahead of print on 18 June 2008.

distinct from the classical lipid rafts (20). However, the biological function of the HCV core protein localized in the DRM has not been clarified.

The HCV core protein is cleaved from a precursor polyprotein by a signal peptidase (SP) to liberate it from the envelope protein E1 and is then further processed by a signal peptide peptidase (SPP) (21). However, the biological significance of the intramembrane processing of the HCV core protein by SPP remains largely unknown. Furthermore, the C-terminal end of the mature HCV core protein expressed in insect cells has been reported to be Phe^{177} or Leu^{179} (12, 29), while that in mammalian cells has not been determined. Expression of SPP enhanced the accumulation of nonenveloped nucleocapsid and reduced that of enveloped nucleocapsid in yeast cells, suggesting that maturation of core protein is carried out after the formation of enveloped particles (17). However, the effect of SPP cleavage on viral assembly in mammalian cells has not been well characterized. Randall et al. have reported that introduction of a small interfering RNA targeted to SPP reduced the production of infectious HCV particles (36), suggesting that SPP is required for the production of HCV particles. In this study, we determined the cleavage site of the mature HCV core protein expressed in human cells and examined the biological significance of the intramembrane processing of the core protein by SPP for the localization of the core protein in the DRM and the production of infectious particles.

MATERIALS AND METHODS

Cell lines and HCV infection. HCV subgenomic RNA was removed from the replicon cell line 9-13 (16) by treatment with alpha interferon. A cell line that was highly permissive for JFH-1 infection was cloned from the resulting crude populations by the limited-dilution method and designated Huh7OK1 (32). The Huh7OK1 cell line retained the ability to produce type I interferons through the RIG-I-dependent signaling pathway upon infection with RNA viruses and exhibited a cell surface expression level of human CD81 comparable to that of the parental cell line. The detailed characteristics of this cell line will be described in a future communication. The HuhOK1 and Huh7.5.1 cell lines (the latter was kindly provided by F. Chisari) and the human embryonic kidney cell line 293T were maintained in Dulbecco's modified Eagle's medium supplemented with 10% fetal calf serum and nonessential amino acids (Sigma, St. Louis, MO). Huh7OK1 or Huh7.5.1 cells were infected with HCV strain JFH-1 as described by Wakita et al. (45). The plasmid carrying strain JFH-1 cDNA under the control of the pol1 promoter (19) was transfected into Huh7OK1 or Huh7.5.1 cells, and propagation of the JFH-1 virus was determined by the production of HCV core protein (as described below) and by the titration of infectious particles (39). The persistently infected Huh7OK1 cells were maintained under normal conditions after 8 passages before use. The 9-13 cell line, which possesses an HCV subgenomic replicon (16), was cultured in Dulbecco's modified Eagle's medium supplemented with 10% fetal calf serum and 1 mg/ml G418.

Plasmids. Genes encoding the N-terminally FLAG-tagged and/or C-terminally hemagglutinin (HA)-tagged core proteins derived from the HCV genotype 1b strain J1 or its mutants were introduced into plasmid vector pcDNA3.1 (Invitrogen, Carlsbad, CA) as described previously (30). Each insert gene was transferred into a pCAGGS vector (28) at the PmeI site. The resulting plasmids encoded the HCV core protein (amino acid residues 1 to 191) with or without FLAG and HA tags at the N and C termini, respectively. All of the core proteins with these tags (FLAG-core-HA proteins) had a mutation of Ala^{191} to Arg in order to prevent cleavage by the SP (7). Plasmid pJH121/JFH-1, carrying a full genomic cDNA of strain JFH-1 under the control of the pol1 promoter, was used to produce the infectious JFH-1 virus (19). An adaptive mutation of Leu to Val at amino acid position 758 in the p7 region was introduced during a long-term passage of the JFH-1 virus into Huh7.5.1 cells (data not shown). To improve the replication efficiency of the JFH-1 virus, a mutation of Leu to Val was introduced into pJH121/JFH-1 by site-directed mutagenesis, and the resulting plasmid was designated pJH121/JFH-1/L758V. To generate plasmids encoding the mutant JFH-1 viruses, the following substitutions were introduced into pJH121/JFH-1/L758V: Val^{139}, Val^{140}, and Leu^{144} were replaced with Ala (JFH-1/VVL/3A); $Ile^{176}$and Phe^{177} were replaced with Ala and Leu, respectively (JFH-1/IF/AL); Ala^{180}, Ser^{183}, and Cys^{184} were replaced with Val, Leu, and Val, respectively (JFH-1/ASC/VLV); and Asp^{2736} was replaced with Asn (JFH-1/GND).

Antibodies and reagents. Antisera against HCV genotype 1 or 2a core proteins were raised in rabbits by immunization with peptides corresponding to the region spanning residues 103 to 115, conserved among genotypes 1a and 1b, or to the region from residue 101 to 119 of genotype 2a (strain JFH-1). These peptides were synthesized and conjugated with keyhole limpet hemocyanin (Scrum Inc., Tokyo, Japan). Antisera were purified with an affinity column conjugated with the antigenic peptides. A monoclonal antibody to HCV NS5A (5A27) was prepared from BALB/c mice (CLEA Japan, Tokyo, Japan) immunized with the recombinant domain I of NS5A by a method described previously (31). Antibodies to caveolin-1, calreticulin, and the FLAG tag (M2) were purchased from Sigma. Antibodies to the HA tag and glyceraldehyde-3-phosphate dehydrogenase (GAPDH) were purchased from Babco (Richmond, CA) and Santa Cruz Biotechnology (Santa Cruz, CA), respectively. The aspartic protease inhibitors $(Z\text{-}LL)_2$ ketone and L685,458 were purchased from the Peptide Institute (Osaka, Japan). These inhibitors were dissolved in dimethyl sulfoxide and stored at −20°C until use.

Transfection, SDS-PAGE, and Western blotting. Huh7.5.1 and 293T cells were transfected with plasmids by lipofection with *Trans* IT LT-1 (Mirus, Madison, WI) and Lipofectamine 2000 (Invitrogen), respectively, according to the manufacturers' protocols. Cells were lysed on ice in Triton lysis buffer (20 mM Tris-HCl [pH 7.4], 135 mM NaCl, 1% Triton-X 100, 10% glycerol) supplemented with a protease inhibitor mix (Nacalai Tesque, Kyoto, Japan) at 24 or 48 h after transfection and were then subjected to sodium dodecyl sulfate-polyacrylamide gel electrophoresis (SDS-PAGE) using Tris-glycine buffer and Western blotting using appropriate antibodies as previously described (30). The stained protein bands were visualized using the SuperSignal West Femto enhanced-chemiluminescence substrate (Pierce, Rockford, IL) and an LAS3000 imaging system (Fuji Photo Film, Tokyo, Japan).

Determination of the expression of the C terminus of the mature HCV core protein in mammalian cells. Two million 293T cells cultured in a collagen-coated dish (diameter, 10 cm) were transfected with pCAGGS-FLAG-core (26) by lipofection, harvested at 20 h posttransfection with a rubber policeman after two washes with ice-cold phosphate-buffered saline (PBS), and collected by centrifugation at 1,000 × g for 5 min. The cells were lysed with 0.1 ml of triple-detergent lysis buffer (45 mM Tris-HCl [pH 7.4] containing 0.5% sodium deoxycholate, 0.1% SDS, 1% Triton X-100, 135 mM NaCl, and a protease inhibitor mix [Nacalai Tesque]) (24). The lysate was stored at −80°C until use. The lysate was thawed on ice and then centrifuged at 20,000 × *g* for 10 min at 4°C. The supernatant was mixed with 20 μl of 50% (vol/vol) anti-FLAG M2 affinity gel (Sigma) and then rotated at 4°C for 90 min. The gel beads were washed with the triple-detergent lysis buffer and then suspended in 30 μl of the loading buffer. The suspended gel beads were boiled for 5 min and then centrifuged at 20,000 × *g* for 5 min at room temperature. The resulting supernatant was subjected to SDS-PAGE, and the gel was stained with Sypro Ruby dye (Invitrogen). The portion of the gel including proteins with an expected molecular size of 20 kDa was excised from the stained gel, washed twice with 200 μl of 50 mM NH_4HCO_3 dissolved in 50% acetonitrile (vol/vol), and then immersed in 100 μl of 100% acetonitrile for dehydration. The dehydrated gel was incubated in 10 mM dithiothreitol and 100 mM NH_4HCO_3 at 56°C for 1 h. To prevent the digestion of Cys residues at the C termini by endoproteinase Asp-N, alkylation of the gels was carried out in 55 mM iodoacetamide and 100 mM NH_4HCO_3 at 25°C for 45 min in the dark. Finally, gel pieces were washed twice with 100 mM ammonium carbonate dissolved in acetonitrile and were dried completely before digestion. An immersed volume of endoproteinase Asp-N solution (10 μg/ml Asp-N and 50 mM NH_4HCO_3) was added to the dried gel and incubated at 37°C overnight, and the supernatant (the digested solution) after centrifugation was transferred to a new centrifuge tube. The precipitated gels were washed first with 20 μl of 20 mM NH_4HCO_3 and then with 20 μl of 50% (vol/vol) acetonitrile in 5% (vol/vol) formic acid, and the washed solutions were mixed with the digested solution and dried completely under a vacuum. The digested mixtures were applied to a ZipTip C_{18} column (Millipore, Tokyo, Japan). After a wash with 0.1% (vol/vol) trifluoroacetic acid, the peptides were eluted with 1 μl of 0.1% (vol/vol) trifluoroacetic acid dissolved in 75% (vol/vol) acetonitrile. Samples with 10 mg of 2,5-dihydroxybenzoic acid per ml of 33% acetonitrile matrix were analyzed by matrix-assisted laser desorption ionization-time-of-flight mass spectrometry (MALDI-TOF MS) using a MALDI-quadrupole-TOF tandem MS (MS-MS) QStar Pulsar *i* system (Applied Biosystems, Foster City, CA) in the linear positive-ion mode following the method of Hitachi Science Systems (Ibaraki, Japan).